

# PROCESSING AND CHARACTERIZATION OF $\text{Al}_2\text{O}_3\text{-Fe/Ni}$ CERME THROUGH EXOTHERM REACTIVE HOT PRESSING

by

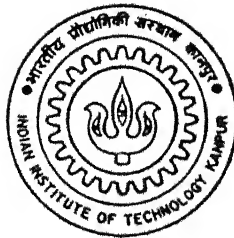
MANAB CHATTERJEE

MME

1995

M

CHA



PRO

DEPARTMENT OF MATERIALS AND METALLURGICAL ENGINEERING  
INDIAN INSTITUTE OF TECHNOLOGY KANPUR

MARCH, 1995

**PROCESSING AND CHARACTERIZATION OF  
Al<sub>2</sub>O<sub>3</sub>-Fe/Ni CERMET THROUGH EXOTHERM  
REACTIVE HOT PRESSING**

248811

*A Thesis Submitted  
in partial fulfilment of the Requirements  
for the Degree of*

**MASTER OF TECHNOLOGY**

*By*

**MANAB CHATTERJEE**

*To the*  
**DEPARTMENT OF MATERIALS & METALLURGICAL ENGINEERING  
INDIAN INSTITUTE OF TECHNOLOGY KANPUR  
March 1995**

18 MAY 1995 / MME  
CENTRAL LIBRARY  
PUR  
119345



A119345

MME-1995-MI-CNA-PRO

DEDICATED  
TO  
MY PARENTS



## ABSTRACT

The conventional method of preparing cermets involve mixing of metal and oxide powders followed by compaction and sintering at elevated temperature with or without application of external pressure. In the present study reactive hot pressing is being utilized where the ingredients are transition metal (Fe) oxide, Al, Ni and / or both Ni and Cr metal powders. The process utilizes the exothermic heat generated during hot pressing to enhance atomic diffusion, thus enabling the fast and intimate sintering of samples. However, the heat generated for a stoichiometric composition is so large that it may melt and deform the samples. This necessitates the addition of excess metal to dilute the heating effect. The process is being tried for the first time and the product material may find its application in rock drilling, rocket nozzle cones etc. The rod-milled powders were characterized with respect to particle size analysis, Differential Thermal Analysis (DTA). The hot pressed pellets were characterized with respect to phase studies and crystallites size by XRD, fractographic microstructure by SEM, Mechanical properties (e.g. indentation hardness, three point bending strength), magnetization behaviour and curie temperautre.

### CERTIFICATE

This is to certify that this work contained in the thesis entitled 'PROCESSING AND CHARACTERIZATION OF  $\text{Al}_2\text{O}_3$ -Fe/Ni CERMET THROUGH EXOTHERM REACTIVE HOT PRESSING' by Manab Chatterjee has been carried out under my supervision and that this work has not been submitted elsewhere for a degree.

 9.3.95  
Dr. K. N. Rai

March, 1995

Professor  
Department of Materials and Metallurgical Engineering  
Indian Institute of Technology Kanpur

## ACKNOWLEDGEMENTS

I wish to express my profound sense of gratitude to Prof. K. N. Rai for his excellent guidance and inspiration in every step of my work.

I am also grateful to Atanuda, Sunuda, Kapurida, Santanuda, Gautamda, Subhas Chand and Dr. Ashok Kumar for their cooperation in my thesis work.

I wish to express my sincere thanks to Shri K. P. Mukherjee, Shri P. K. Pal, Shri A. Agnihotri, Dr. M. N. Mongole, Shri B. Sharma, Shri B. K. Jain, all other staff of MME, MSP and ACMS for their help and cooperation through out the course of this work.

I must thank Shri Yash Pal for an excellent job of typing the thesis and Shri B. K. Jain, for drafting the figure.

I was fortunate to have friends like Ivan, Debangshu, Arnab, Ali, Binod, Shrabani, Sangeeta, Raja and Seniors like Ranganda, Mama, Mami, Kishoreda, Bisuda, Sathpathida, Phoolda, Soumyada, Shymalda, Mimda, Girida, Sandipda, Baruda, Prasenjitda, Gourda, Tapoda, Kachida who have made my stay at IIT Kanpur pleasant and memorable in many ways.

**MANAB CHATTERJEE**

# CONTENTS

Page No.

Abstract

List of Figures

List of Tables

<b>Chapter 1</b>	<b>INTRODUCTION AND LITERATURE REVIEW</b>	<b>1</b>
1.1	Introduction	1
1.2	Cermets	14
1.3	History of Cutting Tool	15
1.4	Sintering Aspects	17
	1.4.1 Mixing effect	19
	1.4.2 Kirkendall Effect	20
	1.4.3 Grain Size Reduction	20
1.5	Statement of the Problem	21
<b>Chapter 2</b>	<b>EXPERIMENTAL PROCEDURE</b>	<b>23</b>
2.1	Chemicals	23
2.2	Preparation of the Pellets	24
	2.2.1 Milling	24
	2.2.2 Hot Pressing	24
	2.2.3 Polishing	25
2.3	Sample Preparation for Mechanical Testing	25
2.4	Sample Preparation for Magnetic Testing	25
<b>Chapter 3</b>	<b>CHARACTERIZATION</b>	<b>26</b>
3.1	Differential Thermal Analysis (DTA)	26
3.2	Particle Size Analysis	27
3.3	Phase Analysis by XRD	28
3.4	Crystallite Size Measurement	29
3.5	Sintered Density Measurement	30
3.6	Porosity Measurement	30
3.7	Measurement of Transverse Rupture Strength (TRS)	30
3.8	Indentation Hardness Measurement	31

3.9	Magnetization Behaviour	31
3.10	Measurement of Curie Temperature ( $T_c$ )	32
3.11	Microstructural Analysis	33
<b>Chapter 4</b>	<b>RESULTS AND DISCUSSION</b>	<b>34</b>
4.1	Particle Size Analysis of the Rod Milled Powder	34
4.2	Differential Thermal Analysis (DTA)	34
4.3	Sintered Density	38
4.4	Porosity	38
4.5	X-Ray Diffraction Studies (XRD)	40
4.6	Crystallite Size	40
4.7	Indentation Hardness	40
4.8	Fractography	44
4.9	Transverse Rupture Strength (TRS)	50
4.10	Magnetization Behaviour	51
	4.10.1 Saturation Magnetization ( $M_s$ )	51
	4.10.2 Remanent Magnetization ( $M_r$ )	51
	4.10.3 Coercivity	54
	4.10.4 Hysteresis Curve (M-H)	57
4.11	Curie Temperature	58
<b>Chapter 5</b>	<b>CONCLUSION AND SUGGESTION FOR THE FUTURE WORK</b>	<b>59</b>
<b>References</b>		<b>61</b>

## LIST OF FIGURES

Number	Title	Page No.
4.1	Variation of the DTA peaks with vol% additive in powder composition	35
4.2	Effect of additive vol% on sintered density and porosity in $\text{Al}_2\text{O}_3$ - Fe/Ni cermet	37
4.3	Variation of XRD pattern with vol% additive in $\text{Al}_2\text{O}_3$ -Fe/Ni cermet	39
4.4	SEM fractographs of $\text{Al}_2\text{O}_3$ -Fe/Ni cermet	45
	<div style="display: flex; justify-content: space-between;"> <div> <p>a. 5 vol% Ni</p> <p>c. 12.5 vol% Ni</p> <p>e. 17.5 vol% Ni</p> <p>g. 15 vol% Ni + 5 vol% Cr</p> <p>i. 15 vol% Ni + 2 wt% <math>\alpha</math>-<math>\text{Al}_2\text{O}_3</math></p> </div> <div> <p>b. 10 vol% Ni</p> <p>d. 15 vol% Ni</p> <p>f. 20 vol% Ni</p> <p>h. 5 vol% Ni + 10 vol% Cr</p> </div> </div>	
4.5	Effect of additive vol% on hardness and TRS in $\text{Al}_2\text{O}_3$ -Fe/Ni cermet	49
4.6	Variation of $M_s$ and $M_r$ with vol% additive in $\text{Al}_2\text{O}_3$ -Fe/Ni cermet	52
4.7	Variation of Coercivity and curie temperature with vol% additive in $\text{Al}_2\text{O}_3$ -Fe/Ni cermet	53
4.8	Effect of vol% additive on the M-H loop in $\text{Al}_2\text{O}_3$ -Fe/Ni cermet	55
4.9	Variation of derivative magnetic moment with temperataure in $\text{Al}_2\text{O}_3$ -Fe/Ni cermet	56

## LIST OF TABLES

Number	Title	Page No.
1.1	Properties of important cutting tool material	17
1.2	Comparison of energies in different methods of sintering	18
1.3	Classification of reactive system	19
2.1	Specification for hot press	24
2.2	Specification of the graphite die punch and sample	24
3.1	Specification for D.T.A.	26
3.2	Experimental parameters used in particle size analysis	28
3.3	Condition of operation for X-ray diffraction	29
3.4	Curie point of ferromagnetic materials	33
4.1	Variation of average particle sizes and DTA peaks with vol% additive in powder composition	36
4.2	Identification of phases and measurement of crystallite sizes by XRD with the vol% additive in $Al_2O_3$ -Fe/Ni cermet	41
4.3	Variation of hardness and TRS with vol% additive in $Al_2O_3$ -Fe/Ni cermet	48
4.4	Variation of magnetization behaviour and curie temperature with wt% additive in $Al_2O_3$ -Fe/Ni cermet.	54

## CHAPTER 1

### INTRODUCTION AND LITERATURE REVIEW

**Abstract :** This chapter mainly reviews the thermite process and application, as our aim of the present study is to synthesize cermet composites based on exothermic reaction. The related subjects where this process can be used are also covered. These are mainly the literature review of thermite reaction, the cermets, the history of cutting tool, the sintering aspects and the statement of the problem.

#### 1.1 INTRODUCTION

In 1900 H. Goldschmidt (1) in Germany performed the aluminothermic reductions, also named 'Thermite reactions' was implemented for the production of Chromium, Tantalum, niobium and other reactive metals from their respective oxides and for the onsite welding of steel rails. The production of uranium from  $Uf_4$  using magnesium also resembles the thermite reactions based on aluminium as the reductant. In recent past lot of works have been done by exploiting the thermite reaction principle on coating, composite fabrication, powder preparation, explosives etc. But in our present case we are interested only the processing of composite fabrication.

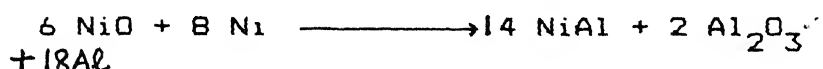
Yokhama et al. [2] have studied the self propagating high temperature synthesis (thermite) centrifugation process in the preparation of large ceramic composite pipes and practical application of the pipes.

Guiseppe et al. [3] have studied the powder metallurgy development of the sintering of Niobium tantalum (NbTa) powders from aluminothermic reduction product (ATR). These powders have



low production costs, procuring data are given as well as the behaviour of the compacts during sintering. Particular emphases is put on sintering parameters, linear shrinkage and specific surface area reduction as well as the analogy of the surface morphology changes.

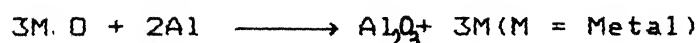
Yamada et al. [4] have studied a new process for intermetallic compounds was developed by combining the thermite reaction and the combustion synthesis reaction. The process enables to produce many compounds. Such as Ni-Ti, Ni-Al and Fe-Al from mixed reactants of metal oxide, metal and/or Semi-metal without external heat supply. In the case of



The combustion temperature exceeds the mp. of both products and the fired NiAl is solidified, Separated from  $\text{Al}_2\text{O}_3$  due to the density difference. This new process could be introduced for casting of intermetallic and ceramic composites.

Odawara et al. [5] have studied the combustion synthesis on the Fe- $\text{Al}_2\text{O}_3$  composite material by thermite process, thermite reaction propagation, residual stress in composite materials, manufacture of composite products and composite pipes.

Odawara et al. [6] has studied the characteristics and development of centrifugal thermite process for fabrication of composite structured pipe.



Propagation of the thermite reaction and preparation of ceramic-ceramic composite - structured pipe by means of the centrifugal thermite process.



Residual stress distribution of the pipe is also analyzed.

Takeda et al. [7] have studied the fabrication process of sintered ceramic materials using heat of thermite reaction and control of their microstructure. The thermochemistry of the thermite reactions, the use of the heat of the thermite reactions to sinter ceramic materials, the control of microstructure of materials densified by thermite - reaction assisted sintering under high pressure and the application of the process to fabrication of  $\text{TiB}_2$  and  $\text{Si}_3\text{N}_4$  are discussed. Microstructural characteristics of the sintered materials in relation to their process condition and applications of the ceramic coating preparation (e.g.  $\text{SiC} - \text{TiB}_2 - \text{NiB}$  etc.) are also discussed.

Odawara et al. [8] have studied the metal - ceramic composite pipes produced by a centrifugal thermite process. Long sized metal - ceramic composites ( $\text{Fe-Al}_2\text{O}_3$ ) pipes were produced by using a thermite reaction that takes place under the influence of centrifugal force. The most important factors that make the production of long composite pipes possibly are the characteristics of thermite reaction propagation. When the reaction is applied to a hollow body, it propagates along the inner surface first and subsequently into the layer of the reactant. By igniting only a part of the reactant, the thermal reaction, rapidly proceeds along the inner surface of the hollow body formed by centrifugal force, and then into the layer simultaneously in the radial direction. The behavior results in the production of long composite pipes of homogeneous quality in the longitudinal direction. The process is discussed with particular reference to the propagation mechanism of the thermite

reaction.

Filatov et al. [9] have studied the effect of intermetallic reactions on combination of nickel - aluminium thermite.

Zhukov, ~~et al.~~ et al. [10] have studied the preparation of cast tool steels by combination of thermite mixtures. The thermite mixtures consisting of  $\text{Fe}_2\text{O}_3$ ,  $\text{WO}_3$ , Al and Carbon black are developed for preparation of liquid tool steel and alloys such as  $\text{R}_{18}$  and  $\text{R}_{18}$  bonded WC. The steel bonded carbide contain 50-60% high speed steel matrix and hence the vickers hardness 1100.

Tada et al. [11] have studied the thermite reaction and mechanical properties of mechanically alloyed aluminium-metallic oxide composites. The thermite reaction and its use in dispersion strengthening of Al was studied in mechanical alloyed Al- $\text{Fe}_2\text{O}_3$ , powder Al- $\text{Cr}_2\text{O}_3$  and Al-  $\text{MoO}_3$  system. DTA shows that the thermite reaction occurs in Al- $\text{Fe}_3\text{O}_4$  at  $> 610^\circ\text{C}$ , where as the reaction is not observed in Al -  $\text{Cr}_2\text{O}_3$  or Al -  $\text{MoO}_3$  at temperature upto melting point of Al ( $660^\circ\text{C}$ ). Dispersion strengthening by thermite reaction products is studied in extrudates of the mechanical alloyed Al- $\text{Fe}_3\text{O}_4$  powder. Annealing  $\geq 610^\circ\text{C}$  increases in hardness and termite strength. The thermite reaction in mechanical alloyed Al- metallic oxide composites is applicable for dispersion strengthening of Al for elevated temperature, services.

Yamazaki ~~et al.~~ [12] have studied the thermite process for metal composite preparation. Between an Fe-oxide-base thermite composition and heating material layers, graphite or an amorphous C based materials is inserted and then the composite is ignited during pressing. Thus in an pyrophyllite - lined die cavity, a Cu-disk (22 mm diam and 3 mm thick) a WC-6% Co compact disc of

6.25 g wt amorphous C 0.6 g, 1.8g of 2:3 mole ratio  $\text{Fe}_2\text{O}_3$  and Si thermite mixture and 25 g of 1:2 mole ratio  $\text{Fe}_2\text{O}_3$  and Al thermite were inserted. The composite was pressed and ignited to prepare a Cu and WC-Co composite.

Odawara et al. [13] have studied the joining of metals to ceramics by self-propagating exothermic reaction, centrifugal thermite method. They have outlined the principles of joining of metals to ceramics by the centrifugal thermite method. Thermite characteristics of the ceramic (inner) - metal (outer) composite tube produced by the centrifugal thermite method under a centrifugal force of 100 - 200 g are also discussed.

Sata Nobwhiro et al. [14] have studied the ceramic lining of metal pipes by thermite process. In this process the metal tubes are cooled from the outside during the reaction. By the cooling treatment, pipes of low melting point, metals can be lined with ceramics. Thus, a brass pipe (id 35.5, length 1.20, wall thickness 4 mm) was packed with mixture comprising 34 g Al and 109g  $\text{Fe}_3\text{O}_4$  and the packing was ignited while the pipe was water cooled to form 3 mm thick ceramic layer.

Sata Nobwhiro et al. [15] have studied the ceramic lining of long steel tube by thermite process. A ceramic layer is formed on the inner wall of a long metal tube by packing a powder mixture of Al and  $\text{Fe}_3\text{O}_4$  into the tube heating the top of packing to initiate the thermite reaction while cooling the tube from outside, repeating the coating process at least twice to join together the coating layers. Thus a graphite saucer was inserted in a C steel tube and a mixture of 195 g Al and 627 g  $\text{Fe}_2\text{O}_3$  was packed into the top part of the tube and ignited while the tube was cooled from

the outside. The same cooling operation was repeated for the rest of the tube to complete the ceramic lining.

Sata Nobuhiro et al. [16] have studied the ceramic lining of steel tubes by thermite process. In lining of steel tubes with ceramics by thermite process, an oxide film is performed on the tubes to increase bonding strength. The a C steel was annealed at  $800^{\circ}\text{C}$  for 0.5 h to form a  $100 - \mu\text{m}$  Fe oxide layer packed with a mixture comprising 117 g Al and 376 g  $\text{Fe}_3\text{O}_4$  and the top of the backing was ignited to initiate the thermite reaction and form a ceramic layer. The ceramic lined tube showed compressive shear stress 3.8 MPa.

Sata Nobuhiro et al. [17] have studied the ceramic coating on the inner wall of metal tube by thermite process. A ceramic layer is formed on the inner wall of a metal tube packing a powder mixtures of Al and  $\text{Fe}_2\text{O}_3$  and/ or  $\text{Fe}_3\text{O}_4$  into the tube, heating the top of the packing to initiate the thermite reaction and forming a thick ceramic layer from the resulting molten metal on the inner wall under control for the tube position. To the powder Al- $\text{Fe}_2\text{O}_3$ - $\text{Fe}_3\text{O}_4$  1-20 wt.% additive from Mg, Al, Si, Ca, Ti, Cr, Fe, Ni, Cu, Zr their alloys and compounds are added to control the thickness and improve the characteristics of the ceramic layer. Thus Al 47,  $\text{Fe}_3\text{O}_4$  177,  $\text{Fe}_2\text{O}_3$  30 and  $\text{SiO}_2$  8g were mixed, press compacted into a C steel tube and the top of packing was ignited by a nichrome wire to initiate the reaction. The reaction slowly progressed from the top to the bottom of the tube to form a 2 mm thick ceramic layer ( $\alpha\text{-Al}_2\text{O}_3\text{-FeAl}_2\text{O}_4$ ).

Sata Nobuhiro et al. [18] have studied the ceramic lining of steel tubes by thermite process. In ceramic lining by thermite

process a partitioning mixture from thick paper wood and powder graphite is used as a marking layer. Thus a hole of 30 mm diameter in the wall of a C steel tube was covered with 5 mm thick paper board layer and thermite mixture of 140g powder Al and 460 g  $\text{Fe}_3\text{O}_4$  was compacted into the tube. In the thermite reaction a ceramic layer was formed only on the unmarked inner wall of the tube.

Filatov, V. M. et al. [19] have studied the thermodynamic analysis of the combustion of the low gas system with a redox stage. An algorithm is proposed for the thermodynamics and of the combination of Al-Ni-NiO thermites by taking into account the formation of aluminides. The adiabatic temperature ( $T_{ad}$ ) and equilibrium concentration of combustion products were calculated as a function of the ratio of the initial components. Maximum  $T_{ad}$  (3140 K) which coincides with the boiling point of Ni was attained in the combustion of a stoichiometric 2 Al + 3 NiO mixtures. The possibility was proven for the formation of  $\text{AlNi}_3$ ,  $\text{AlNi}$  and  $\text{Al}_3\text{Ni}$  is the combustion wave depending on the ( $T_{ad}$ ) and composition of the initial mixture.

Odawara et al. [20] have studied the manufacture of composite pipes. Thin walled steel pipes (wall thickness < 3 mm) are lined with ceramics by thermite reaction. The amount of thermite is determined by the pipe dimensions. Thus thermite mixture containing 15Kg Fe oxide and 5 Kg Al was coated on the inner wall of a steel pipe having diameter 165.2 mm, wall thickness 2.0 mm and length 1430mm. Reaction of thermite was initiated as the pipe was revolved about its axis at 100 g. A ceramic lining was formed without cracked and showed uniform thickness.

Odawara et al. [21] have studied the manufacture of composite pipes by thermite reaction on the inner wall of a pipe under centrifugal rotation. Thermite mixt contains Fe oxide and Al in theoretical ratio with the addition of powder  $\text{Si}_3\text{N}_4$  and/or  $\text{SiC}$  at 1.5-4% of Si. Thus a thermite mixture containing  $\text{Fe}_2\text{O}_3$  1420, Al 480 and  $\text{Si}_3\text{N}_4$  100g was uniformly coated on the inner wall of a steel pipe having outside diam 101.6, wall thickness 42 and length 250 mm. Thermite reaction was initiated in the coated pipe at 1400-1500 r.p.m. Ceramic lining ~ 4 mm thick was formed on the inner wall. The lining containing  $\text{Al}_2\text{O}_3$  87.9,  $\text{SiO}_2$  76 and  $\text{FeO}$  4.5% showed porosity of 2.4%, vickers hardness 1250 and bending strength  $1430 \text{ Kg/cm}^2$  corrosion loss 20% (in 10%  $\text{H}_2\text{SO}_4$ ) of a similarly formed lining from thermite mixture containing  $\text{Fe}_2\text{O}_3$  1390, Al 470 and  $\text{SiO}_2$  140g.

Ogata Masasu et al. [22] have manufactured ceramic metal joined body. The metal ceramic joining body is prepared by forming a ceramic powder layer and a thermite layer on the surface of a metal body and forming a ceramic sintered layer by firing the thermite layer under pressure. A ceramic layer from  $\text{SiC}$  powder with addition of 0.5 wt% graphite powder as the sintering aid was formed on the surface of a Ni plate, then a thermite layer from Al and  $\text{Fe}_2\text{O}_3$  at mole ratio 2:1 was formed on the top of the ceramic layers. The resulting Ni plate was kept at 1 GPa and the thermite layer was ignited by passing electric current through a Mo wire. After firing for 2 minutes a ceramic sintered layer was strongly bonded on the Ni plate.

Takeda et al. [23] have manufactured Silicon nitride sinter of high hardness and density. A high hardness, high density  $\text{Si}_3\text{N}_4$

sintered body is manufactured by packing a thermite reaction. Composition containing Al or Si and  $\text{Fe}_2\text{O}_3$  together with a  $\text{Si}_3\text{N}_4$  molding in an ultra high pressure-generation apparatus at  $> 16\text{GPa}$ , pre sintering the molding by the thermite reaction and sintering for 5-30 minutes at  $1600-2000^\circ$  and  $> 16\text{GPa}$ . Thus a  $\text{Si}_3\text{N}_4$  sintered body manufactured by the present method using a 2:1 (by mole) Al- $\text{Fe}_2\text{O}_3$  mixt as the thermite reaction composition had relative density 98-99% and hardness 1800-2100  $\text{Kg/mm}^2$ .

Odawara et al. [24] have studied the lining of steel pipe with a metal layer and ceramic layer by a centrifugal thermite process. A portion of  $\text{Fe}_2\text{O}_3$  or  $\text{Fe}_3\text{O}_4$  in the thermite mixture is replaced with  $\text{Cr}_2\text{O}_3$ , MnO and/or  $\text{MnO}_2$  which are not readily reducible. A steel pipe (diameter 101.6, thickness 4.2, length 250 mm) was filled with a thermite mixture. Containing  $\text{Fe}_2\text{O}_3$  1076,  $\text{Cr}_2\text{O}_3$  256, Al 512 and  $\text{SiO}_2$  36 g and then ignited while rotating to form a ceramic layer containing 51% FeO.

Odawara et al. [25] have lined a metal pipe with a thermite mixture containing a metal reducing agent and metal oxides and the pipe is axially rotated and ignited to form a metal layer and a  $\text{SiO}_2$ - $\text{B}_2\text{O}_3$ -based ceramic layer. A 165.2 mm diam and 1500 mm long steel pipe was rotated at 1200 rpm and  $\text{SiO}_2$ - $\text{B}_2\text{O}_3$  mixture 2kg, and Al 4.8Kg were charged in the pipe and ignited. The resulting liner had 5mm thick metal and 4mm thick  $\text{Al}_2\text{O}_3$ - $\text{SiO}_2$ - $\text{B}_2\text{O}_3$  ceramic layer.

Sata Nobuhiro [26] has studied the fabrication of plate-or tubular form ceramic materials by thermite reaction. A metal plate or metal pipe for cooling purpose is arranged inside a hollow body and a powder mixt containing a strongly reducing



element and metal oxide (S) is press compacted at a packing density of  $\geq 1.0 \text{ g/cm}^3$  into the hollow body or metal pipe. Then the packed material is heated from its top and the reaction proceeds from the top to bottom while melted material is always contacted with the cooling metal surface to form a ceramic layer between the surface of molten material and the cooling material. It is then cooled and the ceramic layer is separated to give a ceramic part. Thus a spinel pipe with uniform thickness was manufactured from an  $\text{Al-Fe}_3\text{O}_4\text{-MgO}$  mixture by the present method.

Park, J. H. et al. [27] have synthesized sialon by using ceramic raw material. A mixture of opalit (amorphous  $\text{SiO}_2$ ) and Al powder was electrically ignited and the resulting material was used to prepare sialon powder. The phases in samples nitrided at  $1400 - 1600^\circ\text{C}$  were  $\beta$  sialon, 15 R - Sialon,  $\text{Al}_2\text{O}_3$  and AlN. Only  $\beta$  - sialon and 15 R-Sialon were present after heating at  $1750^\circ\text{C}$  for 3 hr in 1 atm.  $\text{N}_2$ .

Ogata et al. [28] have studied the sintering process of metal/or ceramic mixt which is reacted under pressure by a thermite reaction, and a cubic BN (CBN) and/or Ta product is placed between the sintering mixt and thermite as a shield. The ceramic is  $\text{TiB}_2$ ,  $\text{ZrB}_2$  or  $\text{HfB}_2$ . Thus a 7g < 325 mesh  $\text{TiB}_2$  was compacted to a 22 mm. disk, which was then sandwiched between two 1:2  $\text{Fe}_2\text{O}_3\text{-Al}$  mixt disks after placing a CBN Shield between the  $\text{TiB}_2$  and thermite disk. The thermite-CBN- $\text{TiB}_2$ -CBN-thermite composite was placed in a CBN anvil cylinder with a pyrophyllite gasket. The anvils were pressed to 20,222atm and the thermite spontaneously ignited and the temp rose to 2590. The product was electrically conductive and had  $\geq 99\%$  relative density which could

not be achieved by a simple sintering method. The knoop hardness of the product was  $4100 \text{ Kg/mm}^2$ . The products are used for tools, wear-resistant materials, neutron shields etc. This method enables to prepare a high m.p. material with grain coarsening in a short period of time and with use of a small amount of energy.

Odawara et al. [29] have studied the ceramic lined composite pipes. A molten metal and molten ceramic layers were formed on the inside of a metal pipe in a centrifugal force field by a thermite process and the thermite mixture contained a highly oxidizing compound and a dense ceramic layer. Thus steel pipes of 93.2mm inside diam and 250 mm long were filled with a thermite mixt while rotating the pipes at 1500-1600 r.p.m.

Thermite mixture contained  $\text{Fe}_2\text{O}_3$  1.297, Al 0.438, Mg 0.065 and  $\text{SiO}_2$  0.090 Kg. The resulting ceramic contained  $\text{Al}_2\text{O}_3$  82,  $\text{SiO}_2$  5, FeO 3 and MgO 10%.

Sismanis et al. [30] have studied the dissolution of micro exothermic alloying addition to cast iron. Cast iron melt is alloyed by ferro alloy powder mixed with Si in proportion to provide an exothermic reaction and filled into a cast iron cylinder made from sorel metal. The conventional alloying elements have either lower (Sn, Sb, Cu, Mn, Si) or higher (Cr, Mo, V, Nb) m.p than the temperature of the cast iron melt. Powder Fe-Mo (~65%) Fe-Cr (65.73%) and Fe-Nb (~65%) were mixed with ~ 98% purity. Si briqueted in sorel metal containing C 4.3, Si 0.18, balance Fe with traces of GP and S. The dissolution and alloying with the powder mixt of the cast iron melt are enhanced, resulting in improved alloying efficiency and more uniform properties due to the heat released by the formation of intermetallies, coin @d

microexothermicity, as compared to the conventional ferro alloy lumps.

Gehrman et al. [31] have studied the vacuum centrifugal thermite process for producing ceramic lined pipes. A vacuum centrifugal thermite process was used to prepare ceramic lined pipes rapidly. The ceramic layer was dense and the grain size was smaller than that produced under atm. pressure, resulting in improved mechanical properties.

Merzhanov A. G. et al. [32] have developed multilayer shell investment molds. To increase tightness and high temperature strength a protective coating is provided for the shell mold exterior. The coating is a thermite mixt consisting of  $\text{CaCrO}_4$ ,  $\text{MgCrO}_4$ ,  $\text{CaCr}_2\text{O}_7$  or  $\text{PbCrO}_4$  - 43-73.6%, Al, Ti, Zr, Mg, Ca, Si or  $\gamma$  as a reducing metal - 6.4-24%. Synthetic pitch 0.6-1% and a solvent 19.4-32.0%. The coating thickness is 0.4-1 of mold wall thickness. After drying the thermite mixt is ignited.

Odawara et al. [33] have studied the additives for thermite enameling agents for metal tubes  $\text{SiO}_2$  is used as an additive for thermite agents for enameling on the inside wall of metal oxide tubes by ignition of repeated coating layers of the agent, to form metal-ceramic layers. (Addition of  $\text{SiO}_2$  towards inner layers were increased on the outer layer). Thus a steel pipe outer diameter 101.6mm, thickness 4.2 mm and length 250 mm) was rotated around its axis at 500 r.p.m. spray coated internally with 1.3 Kg thermite containing 30 wt%  $\text{SiO}_2$ , then with 0.5 Kg containing 5 wt%  $\text{SiO}_2$  ignited with its inner layers for thermite reaction and cooled. The surface was smooth and solid without porosity.

Odawara ~~et al.~~ et al. [34] have studied the characteristics

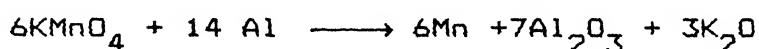
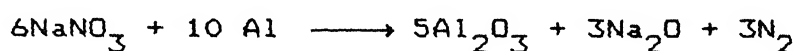
of thermite reaction in a centrifugal thermite process by measuring propagation patterns of reaction in the pipes with various powder densities and shapes. The propagation patterns of reaction in a centrifugal thermite process are also measured by means of a radio telemeter technique. The propagation rate of the thermite reaction is inversely proportional to the thermite powder density. If the reaction is applied to a hollow body, it propagates along the inner surface fast and then into the layer of the reactant subsequently. The hollow body first and then into the layer in the radial direction, resulting in producing the composite pipes of homogeneous quality.

Janikh <sup>1</sup> [35] have reviewed the development of aluminothermic welding technology in the building industry. It consists of the principal and operating procedures for aluminothermic (AT) welding by a mixt of Al and  $\text{Fe}_2\text{O}_3$  with emphasis on joining of concrete reinforcement have been discussed.

Agency of Industrial Science and Technology Kubota Ltd., and Mitsubishi Mining and Cement Co. Ltd. Japan Kokai Tokkyo Koho have studied [36] the formation of acid resistant ceramic layer on the inner surface of concrete pipes. A powder mixture of strongly reducing element and metal oxide is packed into a porous concrete pipes and ignited while rotating to form acid - resistant ceramic layer. Thus a concrete pipe (porosity 3.5%, inner diameter 140, pipe length 200 mm) was packed with Al 140 and  $\text{Fe}_3\text{O}_4$  460g rotated and ignited to form a 2-3 mm thick acid-resistant ceramic layer.

Feichtinger et al. [37] have studied the powder materials for oxidation and heat resistant layers, linings and shape bodies and apparatus for applying this material. A powdered mixture

consisting of a thermite containing Al 5-22%  $\text{KMnO}_4$  3-16% and  $\text{NaNO}_3$  2-12% and filler containing SiC 25-86%,  $\text{H}_3\text{Bo}_3$  10-15% and Kieselguhr 1-5% used for the autothermal coating of graphite electrodes with heat and oxidation resistant SiC - filled  $\text{Al}_2\text{O}_3$  layer. The contents of the thermite and filler in the initial powder are 10-30% and 70-90% respectively. The thermite is composed of Al grains coated with  $\text{KMnO}_4$  and  $\text{NaNO}_3$  by a wet coating process and the filler is composed of SiC grains coated with  $\text{H}_3\text{Bo}_3$  (flux) and kieselguhr, (desensitizer). The thermite filler mixture is sprayed on the sand blasted graphite electrodes preheated to  $390^\circ$  thus initiating the exothermic reaction.



Resulting in the formation of a sintered layer with high oxidation resistance at  $>2000^\circ\text{C}$ . The initial mixture can also be heated and sintered in a mold for the preparation of heat resistant shape bodies.

Kuluba et al. [38] have studied the structural analysis of chromium diffusion layers prepared on steel 45 by the alumino thermic method. The study includes the chemical and phase composition and structure of Cr coating prepared on steel 45 by the alumino thermic method at 1500 K during 2h, using a powdered mixture containing Al,  $\text{Al}_2\text{O}_3$  and  $\text{Cr}_2\text{O}_3$ . The coating contained two solid solution  $\alpha$  and  $\gamma$  and carbide phase  $\text{M}_7\text{C}_3$ . The precipitated phase consisted of Cr 56%, Fe 34% and C 10%. The amount of Cr, Fe and C in the coating matrix was 13.4%, 8.6% and 0.6% respectively. At a given diameter of the sample and cooling in air, the coating had the martensitic structure with residual austenite.

## 1.2 CERMETS

Cermets in the original meaning of the word are composite materials that combine the wear resistance and hardness of the ceramic component with the toughness of the ductile binder metals. Cermet materials containing a ceramic matrix with dispersed metallic particles or metallic fibers are generally mechanically stronger than pure ceramic bodies. Ductility, fracture strength, impact strength, tensile strength and flexural strength are often enhanced.

Several attempts have been made to define [39] cermets. The ASTM committee C-21 has suggested the acceptable following definition : 'A heterogeneous combination of metal(s) or alloy(s) with one or more ceramic phases. In fact cermets are a very broad class of materials including for instance oxide-metal, carbide-metal, nitride-metal, boride metal, sintered systems and even non-metallic compounds -  $\text{SiC}$ ,  $\text{Si}_3\text{N}_4$ ,  $\text{BN}$ ,  $\text{B}_4\text{C}$  - metal systems.

## 1.3 HISTORY OF CUTTING TOOL

The young history of cutting tool reflects the continuing quest towards the ideal, both harder and toughest material - our 20th century challenge corresponding to the old alchemist's dream of lead transmutation into gold, the philosopher's stone. We know now that the stone cannot exist and that hardness and toughness are antagonistic properties. The materials engineer is condemned to seek a compromise between hardness and toughness and this opens up a wide field of investigation. The history of cutting tools can be related in terms of three major families.

- a. Cemented carbides
- b. Cermets

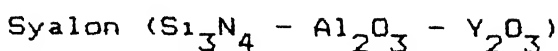
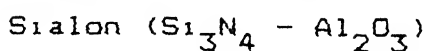
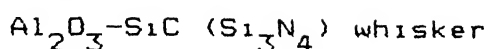
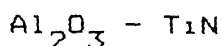
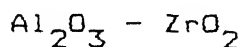
### c. Ceramics and miscellanea

The first improvement in cutting tools occurred in 1906 with the development of high speed steels (HSS). HSS cutting tools were harder than the plain carbon steels then in use and could operate at the faster rate of 30 m/min. With the birth of cemented carbide family in 1923 and after a number of years devoted to improvements (1923, 1950), speeds four times the operating rate of HSS tools were attained 150 m/min. Today the maximum seems to be reached with a rate of 250 m/min for some grades. The most important event since 1923 occurred in 1969 with the launching of coated cemented carbides which very rapidly allowed to work at a rate of up to 500 - 600 m/min [40].

It is interesting to note that the cermets family came on the scene in 1919-1921 before cemented carbides. A lot of grades have since been developed on the basis of carbides, borides and nitrides of transition metals with metallic binders mainly iron group metals. The ceramics family is quite old the first alumina cutting tool appeared in 1930. However, the growth of ceramic tools, mainly based on  $Al_2O_3$ , remained very low until the new era which dawned in the early 1980's and is still unfolding. This is the era of silicon nitride based ceramics. The tools can operate at a speed more than 5 times than that of cemented carbides 800m/min and even 2000 m/min and are not made from strategic materials as are most carbide tools.

Synthetic diamonds were synthesized in the mid 1950's and their development dates from 1980. Diamond tools can be used at twice the speed of cemented carbides - 300 m/min. Synthetic cubic boron nitride was prepared in the late 1950's and is also being

developed since 1980. During the last ten years new material have been proposed.



Properties of some important cutting tool materials are given in Table 1.1.

**Table 1.1 : Properties of important cutting tool materials**

Cutting tool material →	HSS	WC-Co	$\text{Al}_2\text{O}_3$	$\text{Si}_3\text{N}_4$	Sialon	CBN
Property ↓						
Room Temp. hardness (HV)	835	1500	1600	2200	1800	>5400
Hardness at 550°C	600	1000	750	1800	1500	2700
Fracture toughness ( $\text{MN/m}^{3/2}$ )	18	13	1.75	5	7	6.3
Transverse rupture strength (MPa)	4600	2000	380	896	828	-
Thermal conductivity ( $\text{W/m}^\circ\text{C}$ )	31	100	8.4	25	20-25	100
Coefficient of thermal expansion (0-1000°C)	$10 \times 10^{-6}$	$4.9 \times 10^{-6}$	$9 \times 10^{-6}$	$3.2 \times 10^{-6}$	$3.2 \times 10^{-6}$	$4.9 \times 10^{-6}$

#### 1.4 SINTERING ASPECTS :

There are many powder metallurgy [41] and ceramics products in which a chemical comprised of mixtures of powders of different phases or coated particles, or of a phase that undergoes a phase



transformation during heat treatment. In some cases, the purpose is to form the product phase in-situ, such as a ferrite. For some such products, it has been learned that superior properties are achieved with pre-reacted powders, and the earlier technique has been supplanted by co-precipitation, freeze -drying and other means to produce greater homogeneity in starting powders. In many ceramics a minor component additive is intended to 'activate' the densification.

There are several distinct differences that arises for some reactive systems. First, the chemical driving force for the reaction can be much larger than the driving force from the pressure, molecular volume product in hot premixing, which is also larger than the driving force in premixture sintering. These are compared in Table 1.2.

**Table 1.2 : Comparison of energies in different methods of sintering**

Comparison of Energies		J/Moles
Chemical R x n	$\Delta h_{\text{chem}} = -RT \ln 10$	$\sim 1200$
Hot pressing	$(30 \text{ MPa})(V_m)$	$\sim 75$
Sinter	$2\gamma_{sv} V_m / 1\mu\text{m}$	$\sim 1$

Secondly, the enthalpy changes that occur can be significant in reactive system. In the reaction between nitrogen and silicon for reaction bonded silicon nitride, the reaction rate must be controlled to avert melting of the silicon because of the heat released. Conversely, for calcination reactions, the endothermic heat of reaction must be provided.

Thirdly, if a gas is involved as a reactant or a product of

the reaction, gaseous permeation through the porosity is required and many therefore control/affect the kinetics.

Fourthly, the volume fraction of reactants and products change with time in reactive systems. If a solid solution forms from two reactants, one of the reactants will disappear. The kinetics models for sintering do not include any variable volume fraction effects for the condensed phases, although qualitative discussions of the sintering of porcelain bodies have made one of the equilibrium phase diagrams to analyze the sintering temperature effects on the composition and volume fraction of the liquids [42].

#### Reactive Systems

A classification of reactive systems is given in Table 1.3.

Table 1.3 : Classification of reactive systems

1.	$A_1 \rightarrow A_2$	Crystallographic phase change - Hedvall effect
2.	$A+B \rightarrow \alpha$	Solid solution
3.	$A+B \rightarrow \alpha+\beta$	Solid solution
4.	$A+B \rightarrow \alpha+\text{Liquid}$	Liquid phase sintering
5.	$A+B \rightarrow A_xB_y$	Compound formation
6.	$A_1+\text{Liquid} \rightarrow A_2+\text{Liquid}$ ( $\beta \rightarrow \alpha$ $\text{Si}_3\text{N}_4$ with liquid)	
7.	$A_{(s)}+B_{(liq)} \rightarrow$	Dental amalgams (disappearing liquid phase sintering)

#### 1.4.1 Mixing Effects :

One of the first obvious problems that arise for mixed particle system is that it may be difficult to achieve the homogeneity desired / required. In mixing particles of two

components, the 'best' mixture is based on binary random statistics. For spinels and ferrites, it has been shown that order of magnitude changes in the sintering and grain growth rate occurs as the average composition is changed from sub to hyper stoichiometric. Consequently local variations in composition due to inadequate mixing can give rise to large local variations in the microstructure development [44].

#### **1.4.2 Kirkendall Effect :**

The most dramatic differences that arise in reactive systems do so because of the large inequality in the driving forces. The formation of Kirkendall porosity has been invoked for the reaction between magnesia and alumina to form spinel, for which the samples undergo a decrease in density as the reaction proceeds.

The other thing is that the pronounced under cutting at the neck of the particles reveal that the surface area increased rather than decreased during the early stages. This is just opposite to that expected and observed for the sintering of single phase system.

Another effect due to chemical transport is that the crystalline lattice is strained by solid solution formation, the strain may cause spontaneous dislocation generation.

#### **1.4.3 Grain Size Reduction :**

Another dramatic effect that has been reported in several systems is of grain size reduction during interdiffusion in reactive systems. This has been observed in the case of barium titanate coupled with lanthium - oxide-doped barium titanate because of the penetration of the inter diffusion zone by lanthana. The one mechanism involves a simple dissolution of barium titanate into the liquid with the assumption that one

micron grain are observed are nucleated and precipitated out of the liquid upon cooling from the sintering temperature.

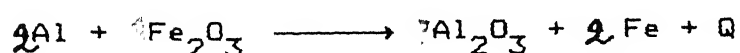
Another instance of grain size reduction has been observed for iron - zinc system [41] . The diffusion induced grain boundary migration and the multiple nucleation of alloy particle along different grain boundaries cause each grain to be penetrated by grain from its neighbours reducing the grain size corresponding by. Alloy formation lowers the free energy sufficiently to exceed the constraint due to grain boundary and curvature, thus driving the system to a higher surface area during the chemical reaction/transient.

#### 1.5 STATEMENT OF THE PROBLEM :

$\text{Al}_2\text{O}_3$ -Fe/Ni composites can be a potential ceramic materials for its attractive mechanical properties in terms of hardness, transverse rupture strength (TRS) and fracture toughness. The development of cutting tool is being persuaded today at a great speed because of the possibility of using them in many application, where they can replace the conventional cutting tool material.

So far considerable amount of work has been done on  $\text{Al}_2\text{O}_3$  as a cutting tool material for its high hardness, transverse rupture strength (TRS) and toughness. No attention has been drawn on the possibility of manufacturing to transition metal based alumina composites using inherent process of thermite reaction. The thermite reaction is very well known in the area of coating and alloying. However its use in making composites suffers from two major debacles firstly, the high exothermic heat containment and secondly the dispersion of low density oxides in the metal matrix.

The excessive exothermic heat has encountered in the thermite application melts the metallic phase completely and leads to complete separation of oxide phase due to glaring density differences. This situation is contradictory to make homogeneous dispersion of ceramic phase into metal matrix. Attempts therefore, have been made in the present investigation to get rid of the above two major difficulties. We have tried to evolve methods for heat containment by adding metallic phases in place of stoichiometric thermite composition to such an extent that exothermic heat is just sufficient to start sintering activity and hold alumina particles generated due to transition metal reduction in the matrix without excessive segregation. The exothermic thermite reaction is shown here.



Thermo reactive hot pressing [44], is also of great interest for making the product. This reactive hot pressing has also been studied by A.C.D. Chakladar and M. N. Shetty [45]. The process has the advantage over the classical hot pressing, in that the driving force for the reaction can also aid densification of the material. Th chemical reaction commonly involves material transport which also has a tendency to accelerate the densification. Due to the extra driving force, it is often possible to sinter materials at temperature lower than that required for normal powder processing. Thermo reactive hot pressing can be particularly advantageous when processing materials which are otherwise difficult to sinter due to low diffusion rates.

In the present investigation powders of  $\text{Fe}_2\text{O}_3$ , Al, Ni and  $\text{Fe}_2\text{O}_3$ , Al, Ni and Cr were taken to synthesize the sample. The evaluation of the products were planned mainly in the area of mechanical properties and magnetic properties.

## CHAPTER 2

### EXPERIMENTAL PROCEDURE

**Abstract :** This chapter discusses the chemicals used in the preparing the composites, preparation of the composites, sample polishing, sample preparation for mechanical and magnetic testing.

#### 2.1 CHEMICALS :

##### 1. Iron oxide red powder ( $\text{Fe}_2\text{O}_3$ )

Source	: LOBA CHEMIC, BOMBAY
Type Analysis	Molecular weight 159.69
Minimum assay	98.5%
Maximum level of impurities :	
Loss on ignition	0.6%
Water soluble matter	0.6%
Other insolubles	0.2%

##### 2. Aluminium metal powder (Al)

Source	: SISCO RESEARCH LABORATORIES PVT LTD.
Fineness	325 mesh
Minimum assay	99%

##### 3. Nickel powder (Ni)

Source	: SISCO RESEARCH LABORATORIES PVT. LTD.
Fineness	100 mesh
Analysis :	
Minimum assay	99.5%
Cobalt	Maximum 0.005%
Iron (Fe)	maximum 0.10%

##### 4. Chromium powder (Cr)

Source	: SISCO RESEARCH LABORATORIES PVT. LTD.
Minimum assay	99%

## 2.2 PREPARATION OF THE PELLETS :

The preparation of the pellets involve the following steps, viz. Milling, hot pressing, polishing.

### 2.2.1 Milling :

The powders of  $\text{Fe}_2\text{O}_3$ , Al,  $\text{Fe}_2\text{O}_3$ , Al, Ni and  $\text{Fe}_2\text{O}_3$ , Al, Ni, Cr were milled (grinding and milling) in a rod mill using steel rods. Acetone was used as a grinding medium. The milling was done for 12 hours. The slurry was dried at  $70^\circ$  for 3-4 hours in an oven.

### 2.2.2 Hot Pressing :

Both pressing and sintering were done simultaneously in a hot press (Dr. Fritsch K.G., Germany) in oxidizing (here, air).

The specification of the hot pressed used is given below:

**Table 2.1 : Specification for Hot Press**

Maker	:	Dr. Fritsch K.G., Germany
Temperature	:	$1200^\circ\text{C}$
Atmosphere	:	Oxidizing
Pressure	:	1 ton
Thermocouple	:	Chromel vs. Alumel
Dia of the pressing rod	:	75 mm

The samples were pressed in the graphite dies at a pressure of 116 MPa.

**Table 2.2 : Specification of the Graphite Die Punch and Sample Graphite Die**

Inner dia	:	10 mm
Length	:	15 mm
Punch dia	:	9.8 mm
Punch length	:	20 mm
<b>Sample</b>		
Sample dia	:	10 mm
Sample thickness	:	5 mm

The sintering temperature was  $850^\circ\text{C}$  and the soaking time was 10 minutes. The pressure was maintained on the sample till it

cools down to room temperature.

### 2.2.3 Polishing :

The hot pressed pellets were then ultrasonically cleaned to remove any trace of graphite. Then after the samples were polished with emery paper of size 0/0, 1/0, 2/0, 3/0, 4/0 and finally on the cloth polishing.

### 2.3 SAMPLE PREPARATION FOR MECHANICAL TESTING :

The each sintered pellets were made half by using the diamond blade and then after from each circular pellets the rectangular samples of sizes 5 mm x 1.5 mm x 2.5 mm were taken out. the samples were then polished with emery paper 0/0, 1/0, 2/0, 3/0, 4/0 and finally with the diamond paste.

### 2.4 SAMPLE PREPARATION FOR MAGNETIC TESTING :

The rectangular samples of size 2 mm x 1.5 mm x 2.5 mm were used for the measurement of Magnetization behaviour and curie temperature ( $T_c$ ).



## CHAPTER 3

### CHARACTERIZATION

**Abstract :** The rod milled powders were characterized by differential thermal analysis (DTA), particle size analysis. The hot pressed pellets phases were evaluated by XRD, crystallite size measurement, sintered density, porosity, transverse rupture strength (TRS), indentation hardness, magnetization behaviour, ~~77°K~~ curie temperature and microstructural analysis.

Each of these methods are presented in this section.

#### 3.1 DIFFERENTIAL THERMAL ANALYSIS (DTA):

Any phase transformation or chemical reaction accompanied by absorption or evolution of heat can readily be detected by DTA.

The specification of DTA - 50 :

**Table 3.1 : Specification of D.T.A.**

Temperature range	:	Ambient temperature to 1500°C
Detector (Thermocouple)	:	Dumbbell type detector (Pt - Pt 10% rhodium)
Measuring range	:	±0.2 to ±1000 GV (with minimum detection sensitivity of S/N = 5)
Noise range	:	0.1 $\mu$ V or smaller
Atmosphere	:	Various gas flow (air, N <sub>2</sub> , O <sub>2</sub> etc at a flow rate of 25 to 50 ml/min) under reduced pressure (about 10 Torr)
Sample Volume	:	About 50 ml
Sample form	:	Substance which is solid or liquid at room temperature
Reference sample	:	Powdered $\alpha$ -Al <sub>2</sub> O <sub>3</sub>
Crucible	:	Platinum

The thermocouples were employed to measure the temperature difference of the test sample ( $T_S$ ) and reference ( $T_R$ ) sample and

hence the temperature difference  $\Delta T = T_S - T_R$ . Platinum crucibles were used instead of  $Al_2O_3$ , both test and the reference sample for its better thermal conductivity.

For exothermic reaction to occur  $\Delta T > 0$  i.e.,  $T_S > T_R$  i.e., thermal conductivity ( $K_S$ ) > Thermal conductivity ( $K_R$ ) and Specific heat ( $C_S$ ) < Specific heat ( $C_R$ ).

For endothermic reaction to occur  $\Delta T < 0$  i.e.,  $T_S < T_R$  i.e., thermal conductivity ( $K_S$ ) < Thermal conductivity ( $K_R$ ) and, specific heat ( $C_S$ ) > specific heat ( $C_R$ ).

DTA of the powders containing,  $Fe_2O_3$ , Al,  $Fe_2O_3/Al/Ni$  and  $Fe_2O_3/Al/Ni/Cr$  were carried out starting from room temperature to  $1000^\circ C$  at a heating rate of  $10^\circ C/min$ . For accuracy of the measurement of the temperature of the transition the weight of the test powder should be less than 200 mg [46].

### 3.2 PARTICLE SIZE ANALYSIS:

Particle size analysis was carried out using Coulter counter model  $Z_B$  and B (Coulter Electronics Ltd., Harpenden Herts, England). particle size analysis was done on the rod milled powders for 12 hours. it gives the number of particles falling in a particular size range. The method applied was dual threshold. The operating condition for the particle size analysis is given in Table 3.2.

Table 3.2 : Experimental Parameters used in Particle Size Analysis

Electrolyte	:	NaCl
Aperture diameters	:	50 $\mu\text{m}$
Manometer volume	:	0.05 cc
Calibration factor	:	1.48
Dispersant	:	Coulter
Gain Control	:	5
Matching switch	:	10

### 3.3 PHASE ANALYSIS BY XRD :

Phase analysis of the rod milled powder and the samples were carried out by x - ray diffraction technique.

#### 3.3.1 Experimental Procedure :

X-ray diffraction pattern ( $2\theta$  vs intensity) of the powder samples were taken with REICH-SEIFERT ISO-DEVYEFLEY 2002 DIFRACTOMETER.  $\text{CuK}_{\alpha}$  ( $\lambda = 1.541846\text{\AA}$ ).

Experimental parameters are given in Table 3.3. X-ray analysis was carried out on the following samples.

All batches of the  $\text{Al}_2\text{O}_3$ -Fe/Ni and  $\text{Al}_2\text{O}_3$ -Fe/Ni/Cr hot pressed pellets.

The x-ray diffraction plots of the samples were measured in  $2\theta$  range of  $20^\circ$  to  $75^\circ$  for phase detection. the d values of the peaks were calculated using Bragg's relation.

$$2d \sin \theta = n\lambda$$

where,

n = order of reflection

$\lambda$  = wave length of radiation

d = interplanar spacing

$\theta$  = diffraction angle

By comparing the d-spacings with ASTM standards the phases presents were identified.

**Table 3.3 : Condition of operation for X-ray Diffraction**

Current, Voltage	:	20 mA, 30 KV
Time constant	:	10 sec
Beam slit width	:	2 min
Detector slit width	:	0.3 mm
Scan speed	:	3°/min
Chart speed	:	3 cm/min
Currents per minute	:	10 K

### 3.4 CRYSTALLITE SIZE MEASUREMENT :

Crystallite size was measured by using the Schenner [47] formula -

$$t = \frac{0.9\lambda}{B \cos \theta_B}$$

where,

$t$  = thickness of crystallite in Å

0.9 = a factor

$\lambda$  = wavelength of X-ray  $\text{CuK}_\alpha$

$\theta_B$  = Braggs reflection angle

$$B = \sqrt{B_M^2 - B_S^2}$$

where,

$B_M$  = width of the peak at the half of the peak height in radian of the material

$B_S$  = Width of the peak at the half of the peak height in radian of the standard sample (here, silicon)

### 3.5 SINTERED DENSITY MEASUREMENT :

The ultrasonically cleaned samples were dried in an oven at 60°C for 12 hrs. The dry weights of the samples were taken by

using an digital electronic balance. The samples were suspended in a distilled water bath and the whole system was kept in vacuum by using rotary pump for about one hour. Repeated checkings were made whether any bubbles were coming from the bottoms on the surface. The weight of the suspended samples were taken while suspended in water (S). Immediately after, the specimens were removed from water, blotted lightly with a tissue paper and weighed in air (W). The sintered density was calculated from the following formulae [48].

$$\text{Sintered density } (\rho_s) = \frac{D}{W - S}$$

### 3.6 POROSITY MEASUREMENT :

The apparent porosities of the samples were measured by using the formulae

$$\text{Apparent porosity} = \frac{W - D}{W - S}$$

Here during this measurement the weight of the suspending wire will have to be taken into account, otherwise it will lead to erroneous result.

### 3.7 MEASUREMENT OF TRANSVERSE RUPTURE STRENGTH (TRS) :

The TRS samples were measured by using three point bending test. The samples of each composition were cut with a diamond blade of thickness 0.4 mm. the size of the samples were approximately 6 mm x 2.5 mm x 1.5 mm. all sides of samples were polished with emery paper 0/0, 1/0, 2/0, 3/0 and 4/0 and finally the diamond polishing were done. TRS of all samples were measured using an Instron 1195 system. The cross head speed was 0.1 mm/min, the chart speed was 20 mm/min and the full scale load was 20 kg.

TRS was calculated by using the following formulae [49]

$$TRS = 1.5 PL/bh^2$$

where,

- P = breaking load in kg  
 L = span in mm  
 b = width of the specimen in mm  
 h = depth of the specimen in mm

### 3.8 INDENTATION HARDNESS MEASUREMENT :

The hardness of the hot pressed compacts were measured by diamond indentation method in the MTS 555 using a load of 20 kg. About five indentations were taken on each polished specimen and the average values of the diagonals were taken into account. Hardness were calculated by using the formulae [50].

$$\text{Hardness} = \frac{2P \sin\left(\frac{\theta}{2}\right)}{L^2} = \frac{1.854P}{L^2}$$

where

- P = applied load, kg  
 L = average length of diagonals, in mm  
 $\theta$  = Angle between opposite faces of diamond =  $136^\circ$

### 3.9 MAGNETIZATION BEHAVIOUR :

The samples of size <3 mm were taken for the measurement of magnetic moment. The samples were measured in the model 155 magnetometer. Magnetic field is increased from 0.017 KOE and the change in the magnetic moments were observed with the continuous increase of the field, the magnetic moment increases.

But it increased to a certain value after that no further increments were observed even highest magnetic field (1.47 KOE). the magnetic moment obtained at that value was saturation magnetization ( $M_s$ ). The magnetic field was decreased gradually and at the point where the field became zero but the material

still had some residual magnetic moment. That point was termed as remnant magnetic moment ( $M_r$ ).

Then after the magnetic field [51] was reversed i.e., the field was applied in the negative direction. The point was reached where the magnetization was zero i.e., to demagnetize the material a field strength ( $H_c$ ) was required which was the coercive force or coercive field of the material. Increasing the field further in the negative direction again produced a maximum induction, but in the opposite direction. The reversal of the field then carried till the saturation magnetization ( $M_r$ ). The closed path so obtained was termed as a hysteresis loop. Its area was an index of the energy loss in a complete cycle of magnetization.

### 3.10 MEASUREMENT OF CURIE TEMPERATURE ( $T_c$ ):

The magnetization of ferromagnetic material depends on the temperature. As the temperature increases the magnetization decreases. Slowly at first and then rapidly until a critical temperature ( $T_c$ ) known as the Curie temperature is reached at which the material is initially non magnetic. This is due to the greater thermal agitation in the lattice at higher temperature tending to break the alignment of atomic magnetic moments. Above the curie temperature the material behaves simply as a paramagnetic material. The Curie temperature has the characteristics value for each magnetic material which is given in the Table 3.4 for related material.

Table 3.4 : Curie Point of Ferromagnetic Materials

Metal	Curie Point ( $T_c$ ) (K)
Iron	1043
Nickel	627.2

A low field 0.15 (KOE) was applied to the specimens and the materials were kept inside the furnace.

The temperature of the furnace was increased and the magnetic moment values were found to be decreased with increasing temperature and with this raw data derivative magnetic moment vs. temperature were plotted. At the point of inflection the slope of the curve became zero was noted as the curie temperature of the materials.

### 3.11 MICROSTRUCTURAL ANALYSIS :

The microstructural analysis of hot pressed  $Al_2O_3$ -Fe/Ni and  $Al_2O_3$ -Fe/Ni/Cr composites containing 5, 10, 12.5, 15, 17.5, 20 vol % Nickel, 15 vol% Ni + 2 wt%  $\alpha$  -  $Al_2O_3$ , (15 Ni + 5 Cr) vol% and (5Ni + 10 Cr) Vol % were done to observe the dispersion of  $Al_2O_3$  in the metal matrix.

The microstructure of these samples were carried out by a JEOL Scanning Electron Microscope (JSM 840 A, Japan). Only fractographic studies were carried out in this present investigation. The photographs were taken in secondary electron image mode (SE) at 5000, 8000, 10000 and 15000 magnification respectively.



## CHAPTER 4

### RESULT AND DISCUSSION

**Abstract :** This chapter mainly presents the results obtained for the particle size analysis of the rod milled powder, differential thermal analysis (DTA) of the powders. The results obtained for the hot pressed compacts are analysed in terms of sintered density, porosity, X-ray diffraction studies (XRD), crystallite sizes, indentation hardness, fractography, transverse rupture strength (TRS). The magnetic properties are considered by magnetization behaviour and curie temperature.

#### 4.1 PARTICLE SIZE ANALYSIS OF THE ROD MILLED POWDER:

Milling of the initial powders are carried out in the rod mill to reduce the particle size for higher densification because fine particle has a higher surface area and hence the higher driving force for sintering. The results of average particle size which is obtained by linear interpolation method is shown in the Table 4.1.

#### 4.2 DIFFERENTIAL THERMAL ANALYSIS (DTA) :

The merit of the DTA curve is that all energy changes occurring in the sample in term of exothermic and endothermic, peaks. The position and the height of the peak decides the temperature at which the process takes place and type (exothermic or endothermic) of reaction. The two different substances may show approximately the same temperature of reaction, the peak area and or shape will be different and although two substances may have the same energy of reaction (and hence the peak temperature) will be different. Because of this each substance gives a characteristics DTA curve which is peculiar to that substance

[46].

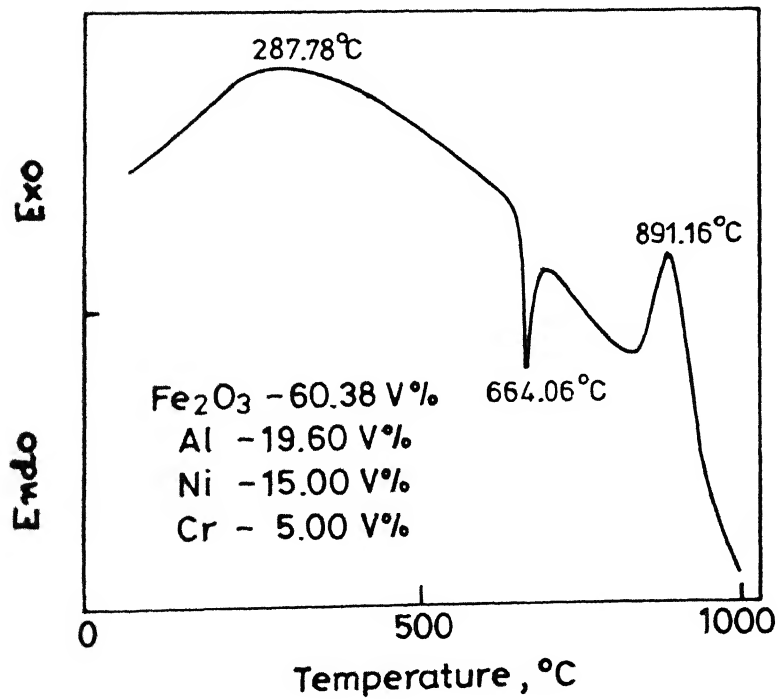
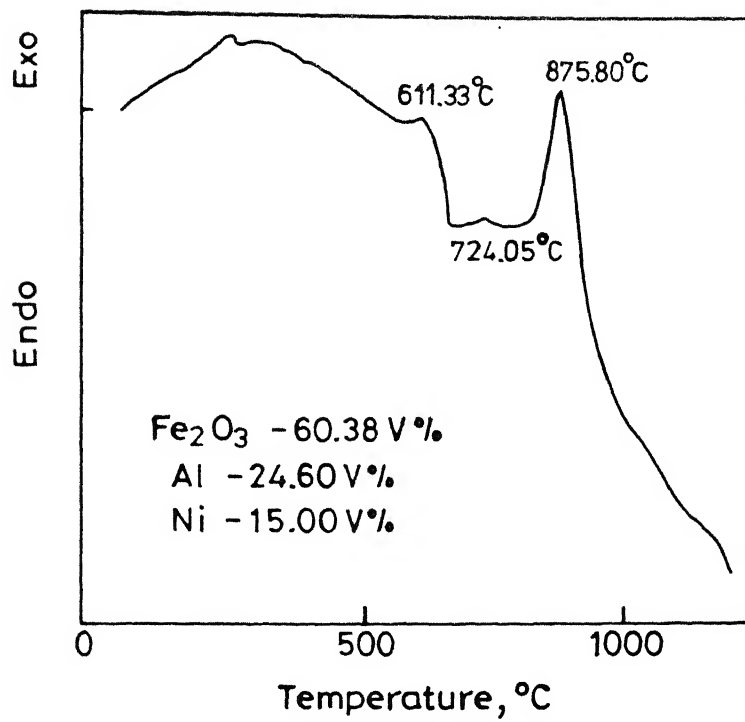


Fig.4.1 Variation of the D.T.A. peaks with vol % additive in powder composition.

Table 4.1 : Variation of Average Particle Sizes, DTA peaks with volume% additive powder composition

Composition (Vol%)				Avg. Particle size ( $\mu\text{m}$ )	Exothermic reaction Temp. ( $^{\circ}\text{C}$ )	Endothermic reaction Temp. ( $^{\circ}\text{C}$ )
$\text{Fe}_2\text{O}_3$	Al	Ni	Cr			
60.38	39.60	-	-	2.53	878.12	695.95
60.38	34.60	5	-	2.01	909.35	669.19
60.38	29.60	10	-	2.53	887.11	680.63
60.38	27.12	12.5	-	2.53	894.20	636.06
60.38	24.60	15	-	1.59	875.80	724.05
60.38	22.12	17.5	-	2.53	882.81	683.36
60.38	19.60	20	-	1.89	893.55	639.87
60.38	19.60	15	5	1.24	891.16	664.06
60.38	24.60	5	10	1.52	883.87	665.57
*60.38	24.60	15	-	1.52	890.11	686.21

\* 2 wt%  $\alpha\text{-Al}_2\text{O}_3$  has also been added

The exothermic peaks for all the powders are observed to be within  $870^{\circ}\text{C}$  to  $910^{\circ}\text{C}$ . It has been observed that with the increasing addition of Ni the exothermic reaction peaks temperature decreases at 5, 10, 15 vol% Ni respectively. But there is a slight increase of exothermic reaction temperature at 12.5, 17.5 and 20 vol% Ni as shown in the Table 4.1. The variation of DTA peaks with vol% additive in powder composition is shown in the figure 4.1. With the addition of Cr the exothermic peaks are observed at  $891.16^{\circ}\text{C}$  and  $883.87^{\circ}\text{C}$ . The addition of 2 Wt%  $\alpha\text{-Al}_2\text{O}_3$  with 15 vol% Ni powder shows the exothermic reaction temperature at  $890.11^{\circ}\text{C}$ . The addition of Cr and  $\text{Al}_2\text{O}_3$  causes sudden increase in reaction temperature. It is felt that the reaction involves the molten Al with  $\text{Fe}_2\text{O}_3$  and metal powders (Ni, Cr) including  $\text{Al}_2\text{O}_3$ . The endothermic peaks are observed for different composition which are varied between  $664^{\circ}\text{C}$  to  $724.95^{\circ}\text{C}$  confirm the solid to liquid transformation of Al.

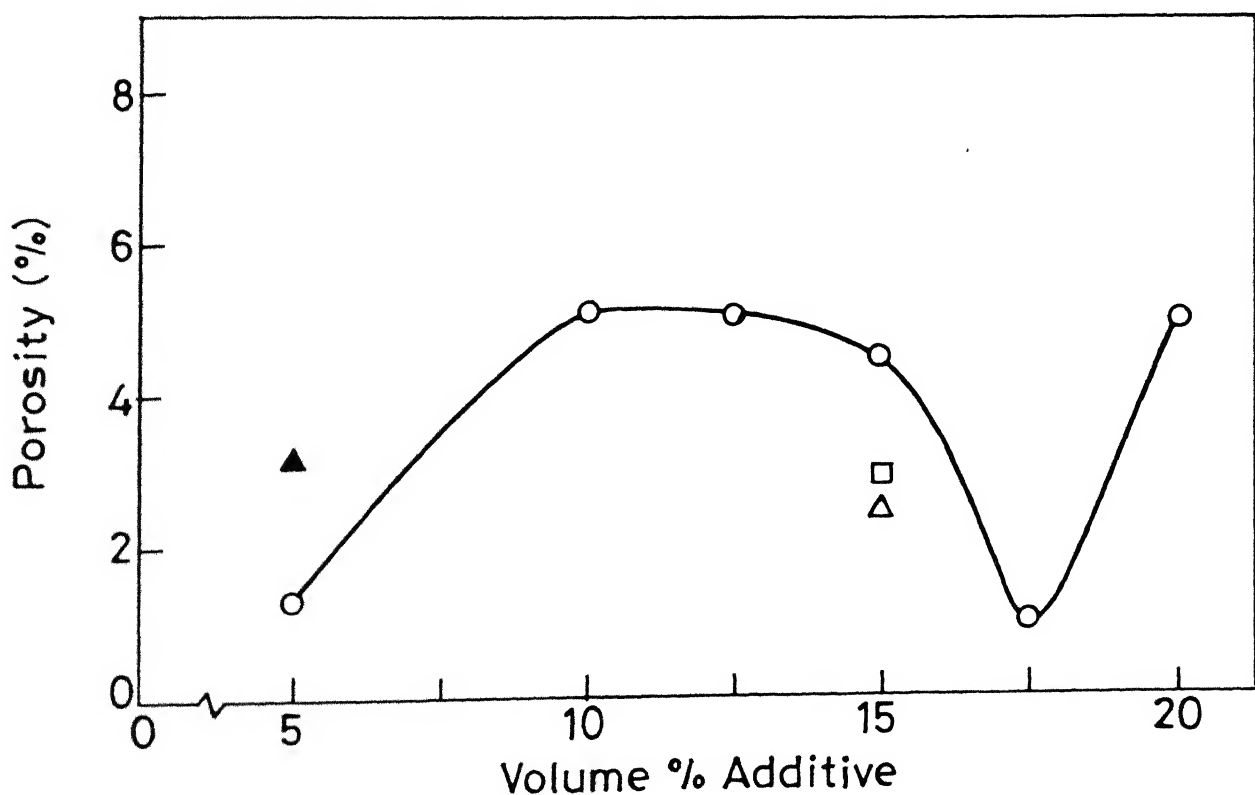
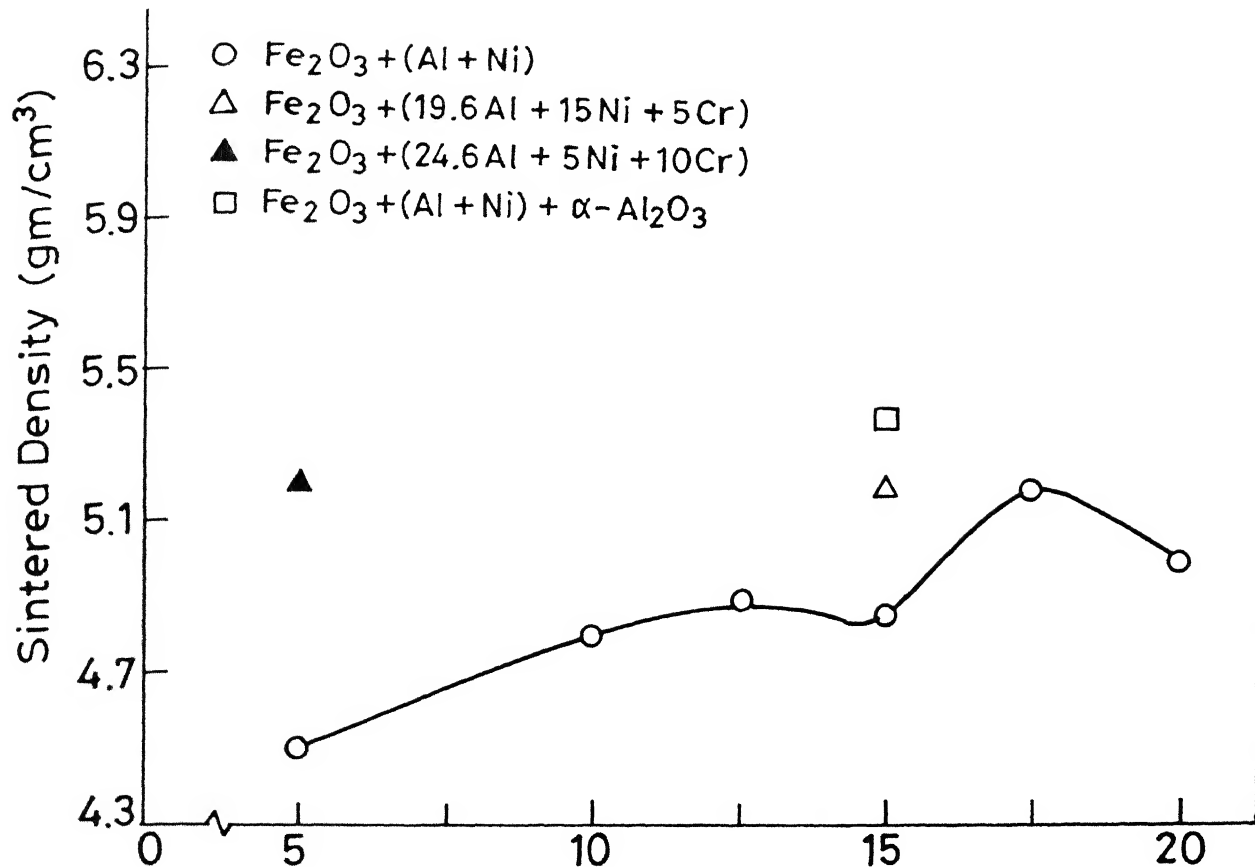


Fig. 4.2 Effect of Vol % additive on sintered density and porosity in Al<sub>2</sub>O<sub>3</sub> -Fe/Ni cermet.

### 4.3 SINTERED DENSITY :

The density of the insitu pelletized pellets are obtained by Archimedes principle. The variation of density of  $\text{Al}_2\text{O}_3$ -Fe/Ni,  $\text{Al}_2\text{O}_3$ -Fe/Ni/Cr composition with the increasing amount of additive (Ni,Cr) is shown in the figure 4.2. From the figure it is observed that the sintered density increases with the increasing addition of Ni from 5vol% to 12.5 vol% . This is expected because the higher density of Ni. There is decrease in density at 15 vol% and 20 vol% Al is replaced by Nickel. The possible reason is the formation of Aluminium Nickel (Al Ni) which does not exist in other composition as detected by X-rays. Aluminium Nickel (Al Ni) has a defect lattice and low density. It changes the lattice parameter according to the Al and Ni vol%.

It is observed from the graph that there is an increase of sintered density with the composition of  $\text{Fe}_2\text{O}_3$ -60.38 v%, Al 19.6 v%, Ni-15 v% and Cr-5 v%,  $\text{Fe}_2\text{O}_3$ -60.38 v% Al-24.6 v% Ni-15 v% and  $\text{Al}_2\text{O}_3$  2 wt%. The possible reason for it the absence of any low density phase as confirmed by X-ray analysis.

### 4.4 POROSITY

The results of porosities measured are presented in the Fig. 4.2. It is observed that the initial composition with 5 vol% Ni additive has the lowest porosity ( $\sim$  1.4%). But with the increase of vol% Ni the porosity increases and it is almost constant  $\sim$  5% to 5.5% at 10 vol% Ni and 12.5 vol% Ni respectively. A decrease in the trend of porosity is observed at 15 vol% Ni and 17.5 vol% Ni. However, the porosity further increases at 20 vol% Ni. The possible reason for the increase of porosity in the compositions containing 10, 12.5, 20 vol% Ni additive is the segregation.

With the addition of Cr and  $\alpha$ - $\text{Al}_2\text{O}_3$  in the 15 vol% Ni, Cr in 5 vol% Ni a decrease in porosity is observed possibly the Cr and  $\alpha$ - $\text{Al}_2\text{O}_3$  promoted densification by decreasing the amount of open pore.

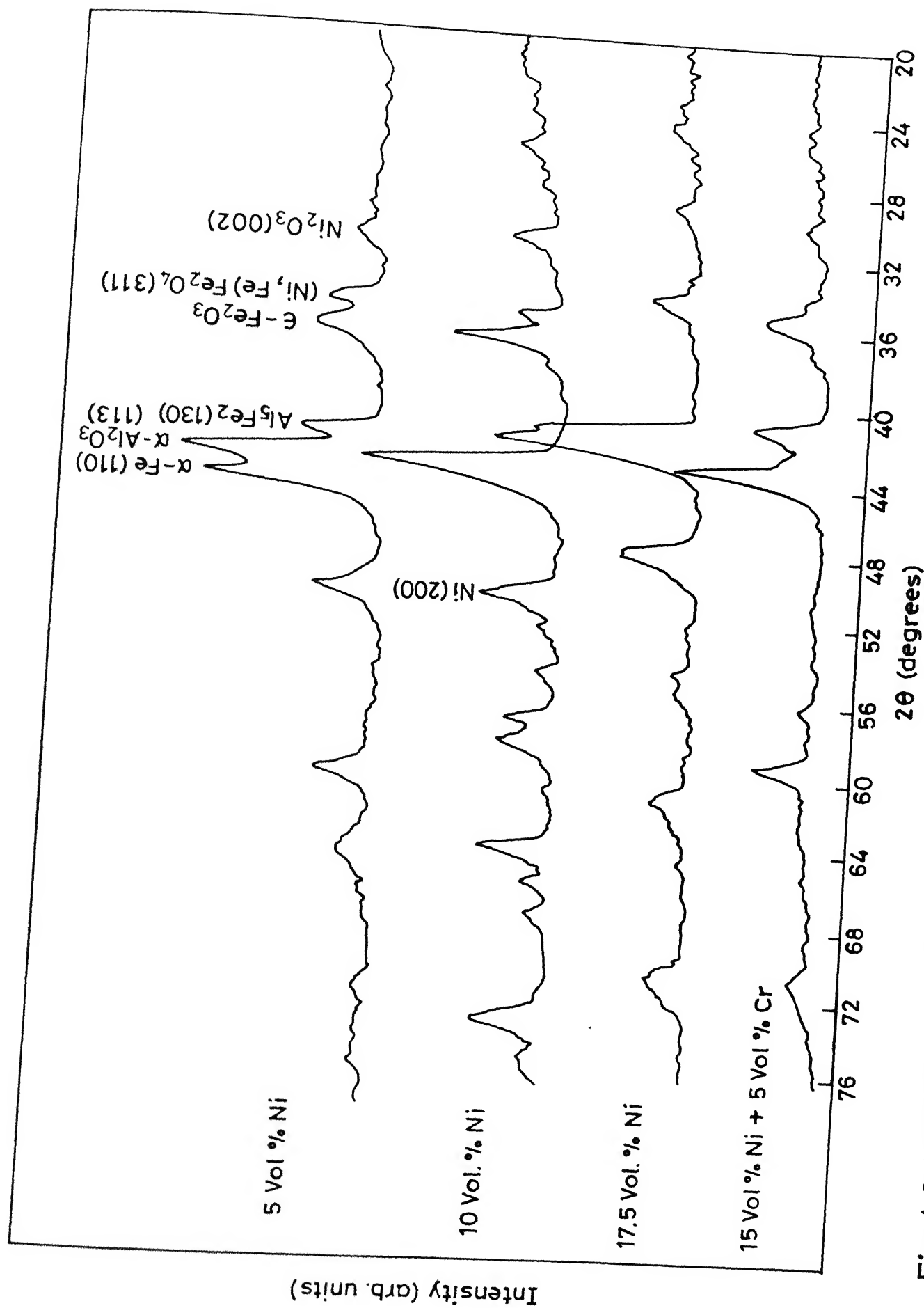


Fig.4.3 Variation of XRD pattern with Vol.% additive in  $\text{Al}_2\text{O}_3$ -Fe/Ni cermet.

#### 4.5 X-RAY DIFFRACTION STUDIES (XRD)

Different phases are detected by X-ray diffractions methods. The diffraction peaks are changed with the change in composition. It is observed that some diffraction peaks are present at certain composition but it is absent in another composition. The phases which are present in different compositions are given in the Table 4.2. The phases are used in interpreting these results in the next sections. The variation of XRD pattern with vol% additive in  $\text{Al}_2\text{O}_3$  - Fe/Ni cermet is shown in the Fig. 4.3.

#### 4.6 CRYSTALLITE SIZE :

The crystallite sizes are measured from X-ray peak broadening by Scherrer formula [47]. Very fine crystallite sizes ( $70\text{\AA}$  to  $180\text{\AA}$ ) are observed. These peak broadening is mainly due to fine crystallite sizes. The value of the crystallite sizes are given in the Table 4.2.

#### 4.7 INDENTATION HARDNESS :

Hardness vs. vol% additive is given in the figure 4.5. It is observed from the figure that hardness values varies between 2.5 GPa to 6.3 GPa. The maximum value of hardness is observed at 12.5 vol% Ni of 6.3 GPa. With the increasing addition of Ni the hardness values increase upto 12.5 vol% Ni. Then after the hardness value is decreased at 15 and 17.5 vol% Ni. However, further enhancement in hardness is observed at 20 vol% Ni. From the X-ray data (Table 4.2) it is detected that  $\alpha$  -  $\text{Al}_2\text{O}_3$  and solid solution  $(\text{Fe,Ni})\text{Fe}_2\text{O}_4$  phases are formed when the vol% Ni is upto 12.5 and only  $\alpha$  -  $\text{Al}_2\text{O}_3$  is formed at 20 vol% Ni. It is clear that the presence of  $\alpha$  -  $\text{Al}_2\text{O}_3$  is responsible for the enhancement in hardness though the solid solution of  $(\text{Fe,Ni})\text{Fe}_2\text{O}_4$  has further effect on hardness. Addition of higher amount of Ni in the case of 15 vol% Ni and 17.5 vol% Ni retard the formation of solid solution phase. The effect of additive volume % on hardness and TRS in  $\text{Al}_2\text{O}_3$  - Fe/Ni cermet is shown in figure 4.5.

Table 4.2: Identification of phases and measurement of crystallite sizes by XRD with vol% additive in  $\text{Al}_2\text{O}_3$ -Fe/Ni cermet.

Composition (Vol%)				Phases (Possible)	Inter-planar spacing (d) (Å)	Intensity I/I <sub>0</sub>	Plane (hkl)	Crystallite size (Å)
Fe <sub>2</sub> O <sub>3</sub>	Al	Ni	Cr					
60.38	39.60	-	-	Fe <sub>2</sub> O <sub>3</sub>	2.7	100	(104)	98.6
				$\alpha$ -Al <sub>2</sub> O <sub>3</sub>	2.085	100	(113)	318.9
				$\alpha$ -Fe	2.03	100	(110)	-
				$\alpha$ -Fe	1.17	20	(200)	-
60.38	34.60	5	-	Ni <sub>2</sub> O <sub>3</sub>	2.80	100	(002)	-
				$\alpha$ -Fe	2.03	100	(110)	-
				(Ni,Fe)Fe <sub>2</sub> O <sub>4</sub>	2.52	100	(311)	-
				$\epsilon$ -Fe <sub>2</sub> O <sub>3</sub>	2.46	100	-	81.06
				Al <sub>5</sub> Fe <sub>2</sub>	2.05	100	(130)	-
				$\alpha$ -Al <sub>2</sub> O <sub>3</sub>	2.085	100	(113)	120.7
				Ni	1.76	42	(200)	-
				$\alpha$ -Fe	1.17	20	(200)	-
60.38	29.60	10	-	Ni <sub>2</sub> O <sub>3</sub>	2.80	100	(002)	-
				(Ni,Fe)Fe <sub>2</sub> O <sub>4</sub>	2.52	100	(311)	-
				$\epsilon$ -Fe <sub>2</sub> O <sub>3</sub>	2.46	100	-	174.
				$\alpha$ -Al <sub>2</sub> O <sub>3</sub>	2.085	100	(113)	88.
				Ni	1.76	42	(200)	-
60.38	27.12	12.5	-	Ni <sub>2</sub> O <sub>3</sub>	2.80	100	(002)	-
				Fe Fe <sub>2</sub> O <sub>4</sub>	2.6	100	( $\bar{1}$ 02)	-
				(Ni,Fe)Fe <sub>2</sub> O <sub>4</sub>	2.52	100	(311)	67.
				$\gamma$ -Al <sub>2</sub> O <sub>3</sub>	1.98	100	(400)	79.
				$\epsilon$ -Fe <sub>2</sub> O <sub>3</sub>	1.43	100	-	-



Table 4.2 (Conttd.)

Composition (Vol%)				Phases (Possible)	Inter- planar spacing (d) (Å)	Intensity $I/I_0$	Plane (hkl)	Crys size (Å)
$Fe_2O_3$	Al	Ni	Cr					
60.38	24.60	15	-	$Ni_2O_3$	2.80	100	(002)	-
				$\epsilon-Fe_2O_3$	2.46	100	-	117
				$Al_5Fe_2$	2.05	100	(130)	-
				AlNi	2.02	100	(110)	-
				$\alpha-Fe$	2.03	100	(110)	-
				Ni	1.76	42	(200)	-
60.38	22.12	17.5	-	$FeFe_2O_4$	2.60	100	(102)	94
				$Al_5Fe_2$	2.05	100	(130)	-
				FeNi	1.87	100	-	-
				$\epsilon-Fe_2O_3$	1.43	100	-	-
60.38	19.60	20	-	$\epsilon-Fe_2O_3$	2.46	100	-	104
				AlNi	2.02	100	(110)	-
				$\alpha-Al_2O_3$	2.085	100	(113)	79
				Ni	1.76	42	(200)	-
				$Al_5Fe_2$	2.05	100	(130)	-
60.38	19.60	15	5	$FeFe_2O_4$	2.60	100	(102)	94
				$AlFe_3C_{0.5}$	2.177	100	(111)	-
				$Al_8Cr_5$	2.146	100	(303)	-
				$\epsilon-Fe$	1.84	100	(101)	-

Conttd...

Table 4.2 (Cont'd.)

Composition (Vol%)				Phases (Possible)	Inter- planar spacing (d) (Å)	Intensity I/I <sub>0</sub>	Plane (hkl)	Cryst size (Å)
Fe <sub>2</sub> O <sub>3</sub>	Al	Ni	Cr					
60.38	24.60	5	10	Cr <sub>3</sub> O <sub>8</sub>	3.80	100	-	-
				Ni <sub>2</sub> O <sub>3</sub>	2.80	100	(002)	-
				(Ni,Fe)Fe <sub>2</sub> O <sub>4</sub>	2.52	100	(311)	96.7
				AlFe <sub>3</sub> C <sub>0.5</sub>	2.177	100	(111)	-
				Al <sub>8</sub> Cr <sub>5</sub>	2.146	100	(303)	-
				α-Al <sub>2</sub> O <sub>3</sub>	2.085	100	(113)	74.4
*60.38	24.60	15	-	Ni <sub>2</sub> O <sub>3</sub>	2.80	100	(002)	-
				ε-Fe <sub>2</sub> O <sub>3</sub>	2.46	100	-	134.1
				α-Al <sub>2</sub> O <sub>3</sub>	2.085	100	(113)	120.
				α-Fe	2.03	100	(110)	-
				Ni	1.76	42	(200)	-

\* 2 wt% α - Al<sub>2</sub>O<sub>3</sub> has also been added.

$$\text{Formula} \quad \% \text{ volume fraction} = \frac{w_i / \rho_i}{\sum w_i / \rho_i} \times 100$$

$$\% \text{ wt fraction} = \frac{w_i}{\sum w_i} \times 100$$

where,  $w_i$  = wt of ith species

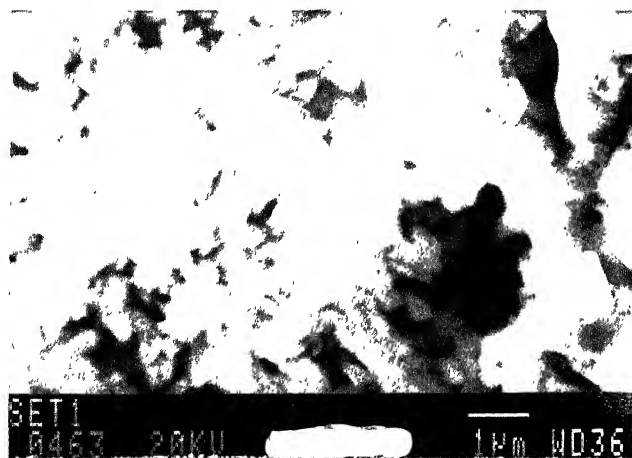
$\rho_i$  = density of ith species

The addition of 5 vol% Cr with 15 vol% Ni, 10 vol% Cr with 5 vol% Ni do not improve the hardness to a considerable extent. The possible cause is the formation of Aluminium iron carbide (AlFe<sub>3</sub>C<sub>0.5</sub>). The carbon has diffused from the graphite die during

hot pressing at high temperature. The addition of 2 wt%  $\alpha$ -  $\text{Al}_2\text{O}_3$  with 15 vol% Ni also does not show any improvement in the hardness. This is due to the absence of solid solution (Fe, Ni)  $\text{Fe}_2\text{O}_4$  phase as it is detected by X-rays. The hardness and TRS values are given in the Table 4.3.

#### 4.8 FRACTOGRAPHY :

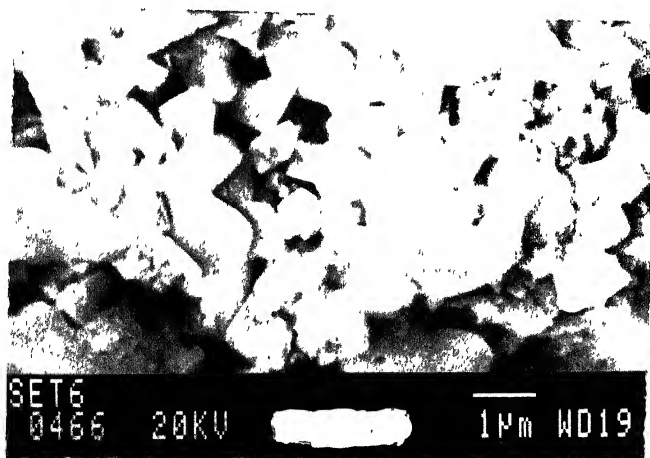
The figure 4.4 show the fractured surfaces of with vol% additive in  $\text{Al}_2\text{O}_3$  - Fe/Ni cermets. Uniform grains are observed in all the composition except when the vol% Ni are 12.5 and 17.5 respectively. The non-uniformity in the grain size distribution in these composition due to the absence of free Nickel. Nickel retards the grain boundary mobility and produces the uniform grain size distribution. At 15 vol% Ni the most uniform microstructure (Fig. 4.4d) is observed. From the figures it is observed that the fracture is semi brittle and semi ductile type [52]. These microstructures have also been used in explaining Transverse Rupture Strength (TRS) variation in the next section.



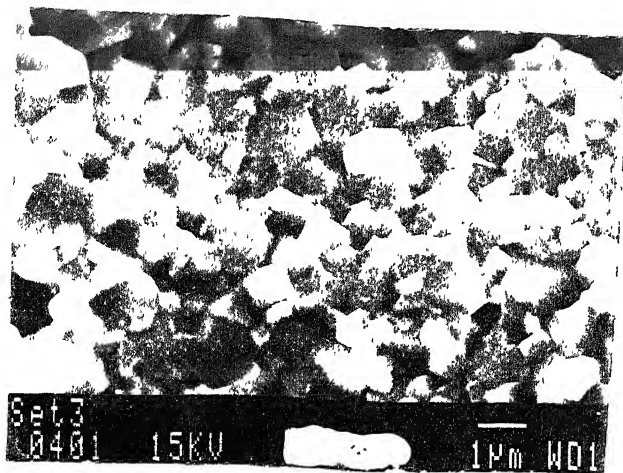
(a)



(b)



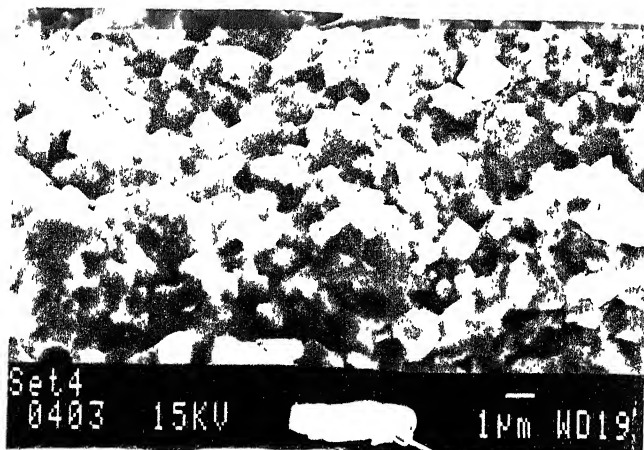
(c)



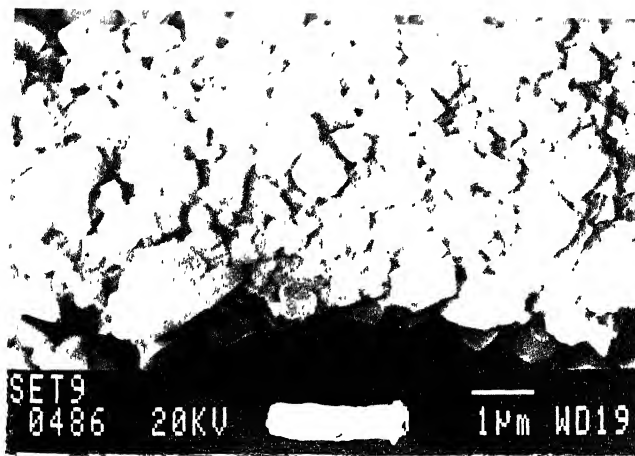
(d)



(e)



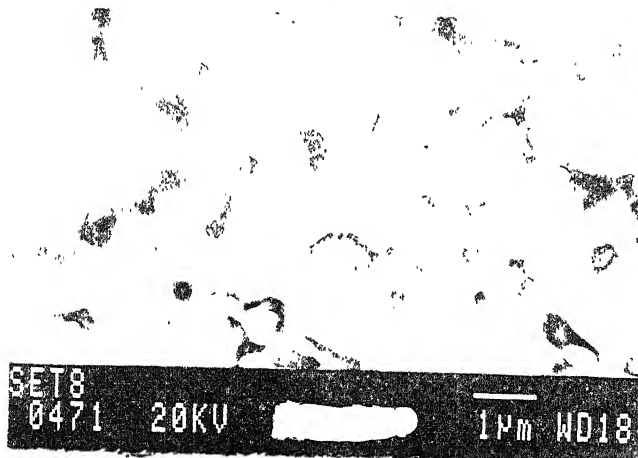
(f)



(g)



(h)



(i)

Fig. 4.4 SEM fractographs of  $\text{Al}_2\text{O}_3$ -Fe/Ni cermet

- |    |                           |    |                           |    |  |
|----|---------------------------|----|---------------------------|----|--|
| a. | 5 vol% Ni                 | b. | 10 vol% Ni                | c. | 12.5 vol% Ni   |
| d. | 15 vol% Ni                | e. | 17.5 vol% Ni              | f. | 20 vol% Ni   |
| g. | 15 vol% Ni<br>+ 5 vol% Cr | h. | 5 vol% Ni<br>+ 10 vol% Cr | i. | 15 vol% Ni<br>+ 2 wt% $\alpha\text{-Al}_2\text{O}_3$ |

Table 4.3 : Variation of hardness and TRS with vol% additive in  $\text{Al}_2\text{O}_3$ -Fe/Ni cermet

Composition (Vol%)				Sintering Temp. ( $^{\circ}\text{C}$ )	Soaking time (min)	Hardness (GPa)	TRS (MPa)
$\text{Fe}_2\text{O}_3$	Al	Ni	Cr				
60.38	39.60	-	-	Could not sintered due to excess exothermic heat	-	-	-
60.38	34.60	5	-	850	10	$4.0 \pm 0.5$	$182 \pm 4$
60.38	29.60	10	-	850	10	$4.6 \pm 0.3$	$187 \pm 3$
60.38	27.12	12.5	-	850	10	$6.3 \pm 0.5$	$106 \pm 7$
60.38	24.60	15	-	850	10	$3.98 \pm 0.1$	$182 \pm 5$
60.38	22.12	17.5	-	850	10	$2.5 \pm 0.1$	$88 \pm 10$
60.38	19.60	20	-	850	10	$5.7 \pm 0.2$	$191 \pm 7$
60.38	19.60	15	5	850	10	$4.8 \pm 0.4$	$87 \pm 10$
60.38	24.60	5	10	850	10	$4.0 \pm 0.6$	$91 \pm 3$
*60.38	24.60	15	-	850	10	$3.8 \pm 0.1$	$145 \pm 5$

\* 2wt%  $\alpha$ - $\text{Al}_2\text{O}_3$  has also been added into it.

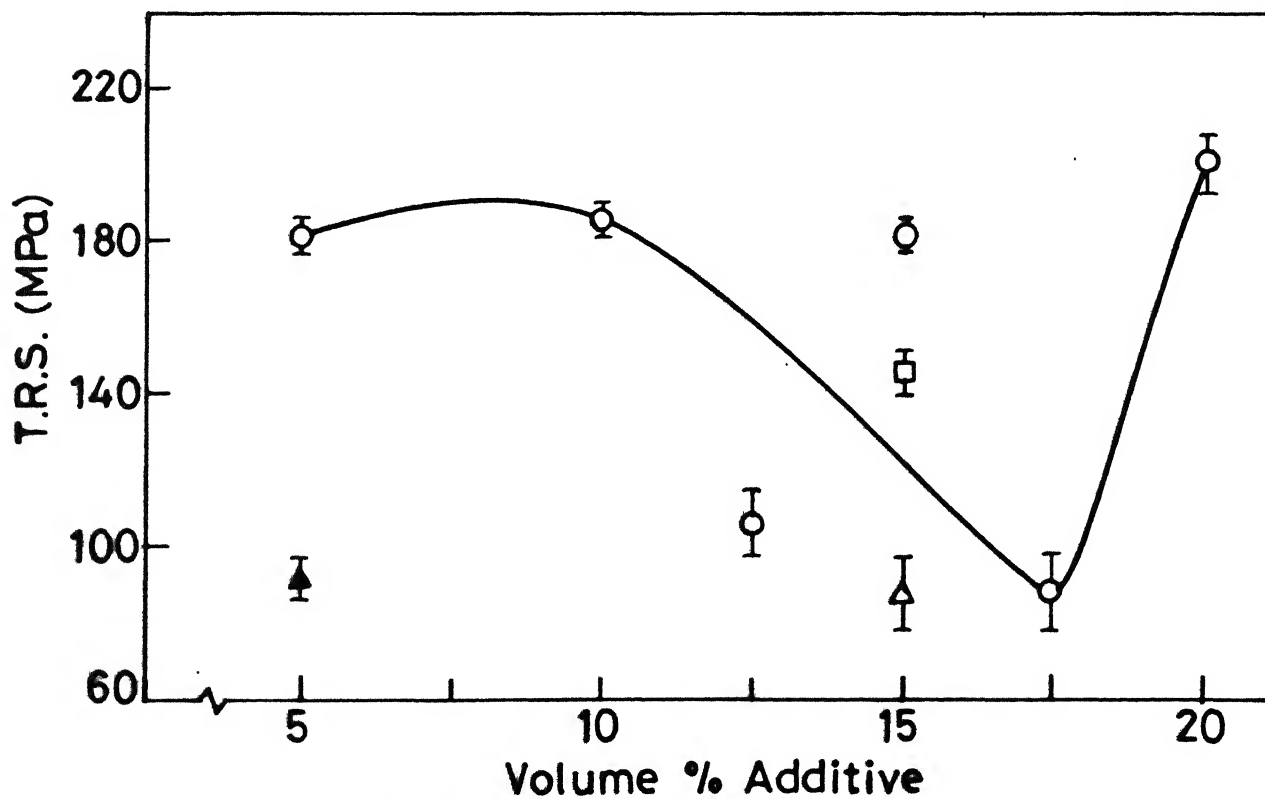
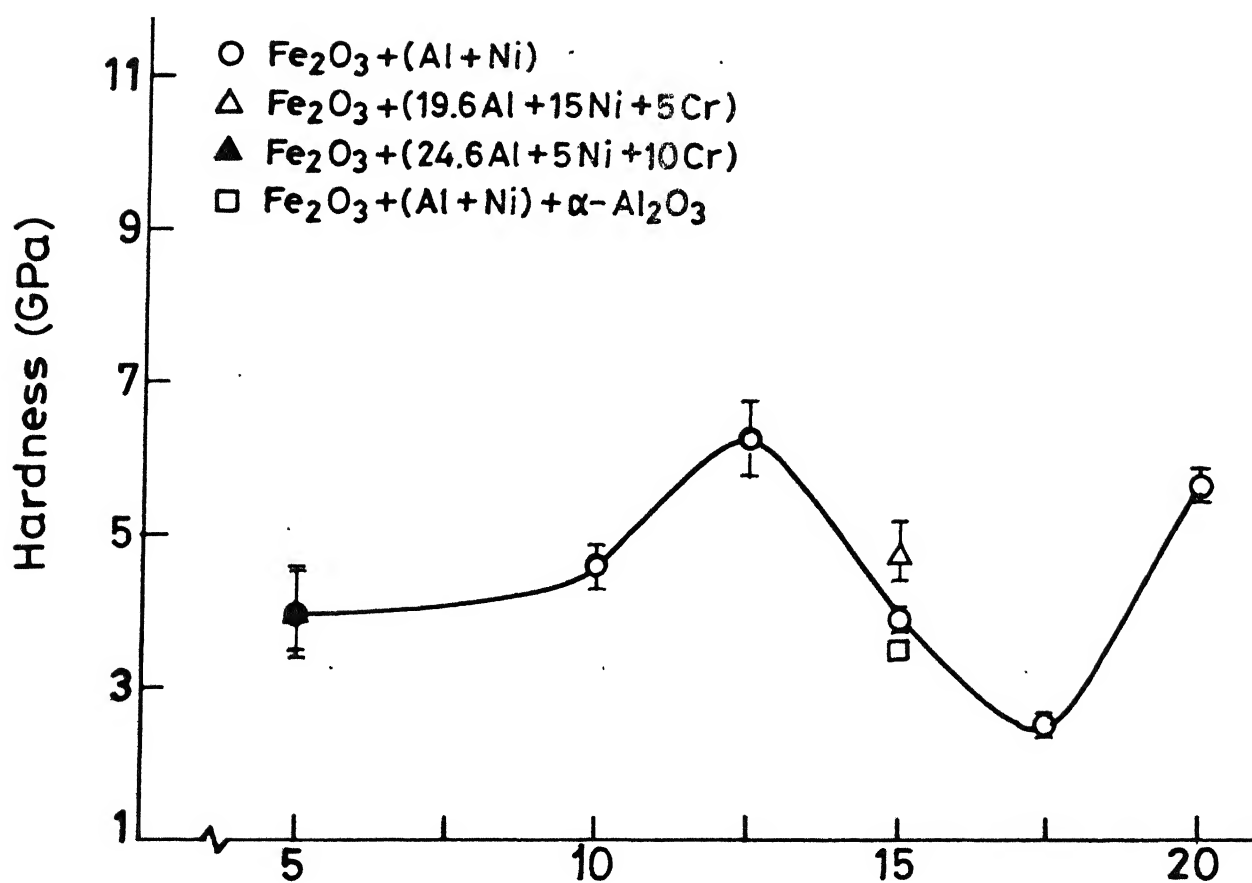


Fig.4.5 Effect of Vol % additive on hardness and T.R.S.  $\text{Al}_2\text{O}_3$  - Fe/Ni cermet.



#### 4.9 TRANSVERSE RUPTURE STRENGTH (TRS) :

The samples containing 5, 10, 15, 20 vol% Ni showing similar TRS values in Fig. 4.5. These samples exhibit microstructure of uniform grain size as shown in the Figure 4.5. However in contrast the samples containing 12.5 and 17.5 vol% Ni exhibit exaggerated grain growth. The decrease in strength in the 12.5 and 17.5 vol% Ni can be explained by Hall and Petch equation [50].

$$\sigma_0 = \sigma_i + kD^{-1/2}$$

where

$\sigma_0$  = yield stress

$\sigma_i$  = friction stress representing the overall resistance of the crystal lattice

k = 'locking parameter' which measures the relative hardening contribution of the grain boundaries

D = grain diameters

Thus the increase in grain diameter leads to decrease in the failure strength of the material. The enhance grain growth occurs in the two composition due to the absence of free Ni. The presence of Ni hinders the grain boundary mobility and produces the uniform microstructure.

At 5 vol% Ni with 10 vol% Cr the TRS values are lowered compared to other composition which is shown in the Table 4.3. This is possibly due to the formation of a brittle  $\text{AlFe}_3\text{C}_{0.5}$  phase as detected by X-rays (Table 4.2). At 15 vol% Ni with 2 wt%  $\alpha\text{-Al}_2\text{O}_3$  the improvement in the TRS value is observed possibly due to the presence of free Fe and Ni which retard the grain boundary movement and produces the uniform microstructure as detected in SEM.

#### 4.10 MAGNETIZATION BEHAVIOUR :

##### 4.10.1 Saturation Magnetization ( $M_s$ ) :

All the results given in the Table 4.4 shows that the saturation magnetization for samples occur at reasonably large field (7.9 Koe to 11 Koe). This is possibly due to the high demagnetizing factors for small specimens. It is observed from the figure 4.6 that there is a increase in saturation magnetization with the increase of Ni except for the 25.856 wt% Ni and 22.21 wt% Ni. The increase in saturation magnetization  $M_s$  (e.m.u./cm<sup>3</sup>) possibly due to the addition of Ni. Nickel increases the average magnetic moment of the alloy because magnetic moment of Ni ( $m_{Ni} = 0.6 \mu_B$ ) [53]. At 22.21 wt% Ni and 25.85 wt% Ni a decrease in the magnetic moment is observed possibly due to the inhomogeneity in the hot pressed material.

The addition of 6.672 wt% Cr with 24.77 wt% Ni and 15.60 wt% Cr with 8.78 wt% Ni decreases the saturation magnetization ( $M_s$ ). Addition of Cr to the  $Fe_2O_3$ -Al-Ni system induces the formation of inhomogeneous inclusion with nonuniform distribution with respect to their shape and size. This inclusion causes either the formation of magnetic poles or a stressed domain structure and thus reduces the value of  $M_s$ . The other possible reason is that Cr does not itself contribute to the ferro or ferrimagnetic moment. Therefore the  $M_s$  value is decreased proportionately.

##### 4.10.2 Remanent Magnetization ( $M_r$ ) :

It is the value of the residual magnetization by the withdrawal of the magnetic field. It is observed from the figure 4.6 that the remanent magnetization decreases with the increasing amount of Ni upto 18.338 wt% Ni and then after it remains almost constant upto 32.522 wt% Ni.

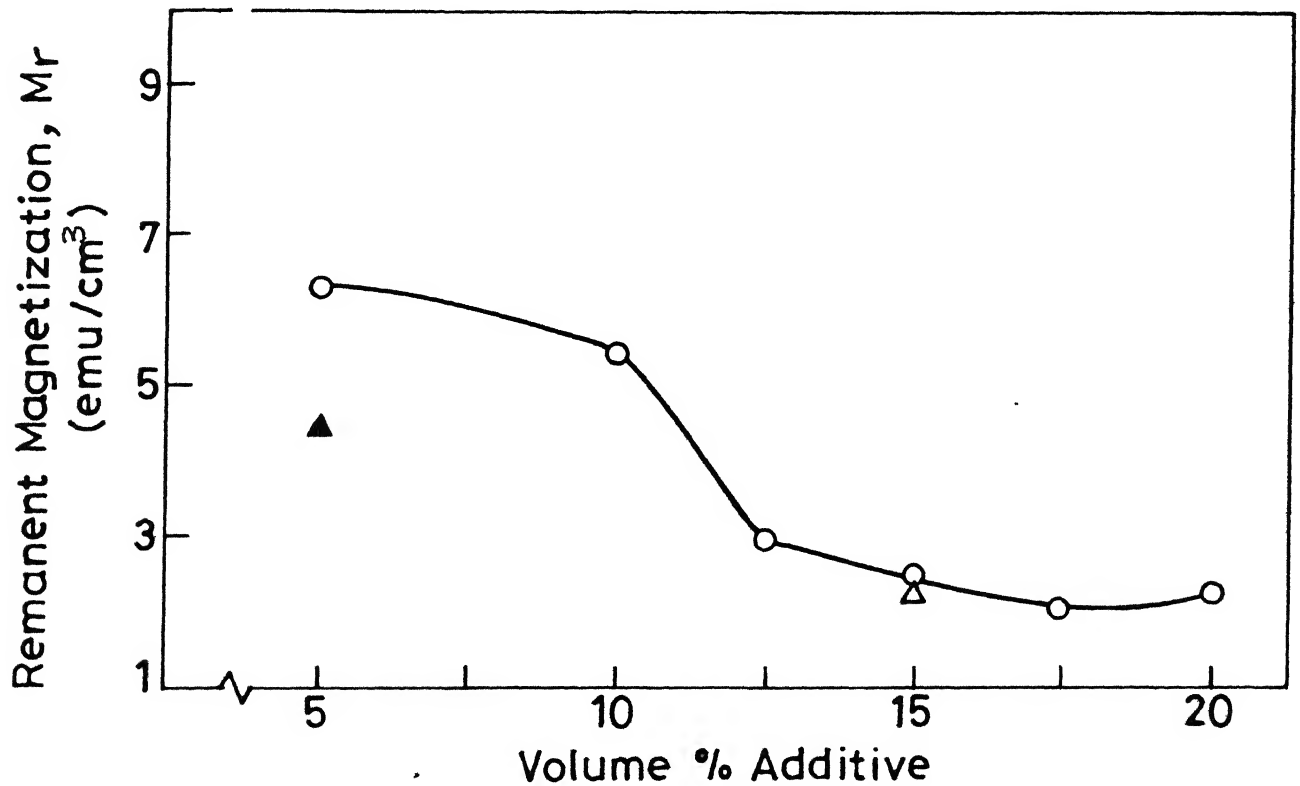
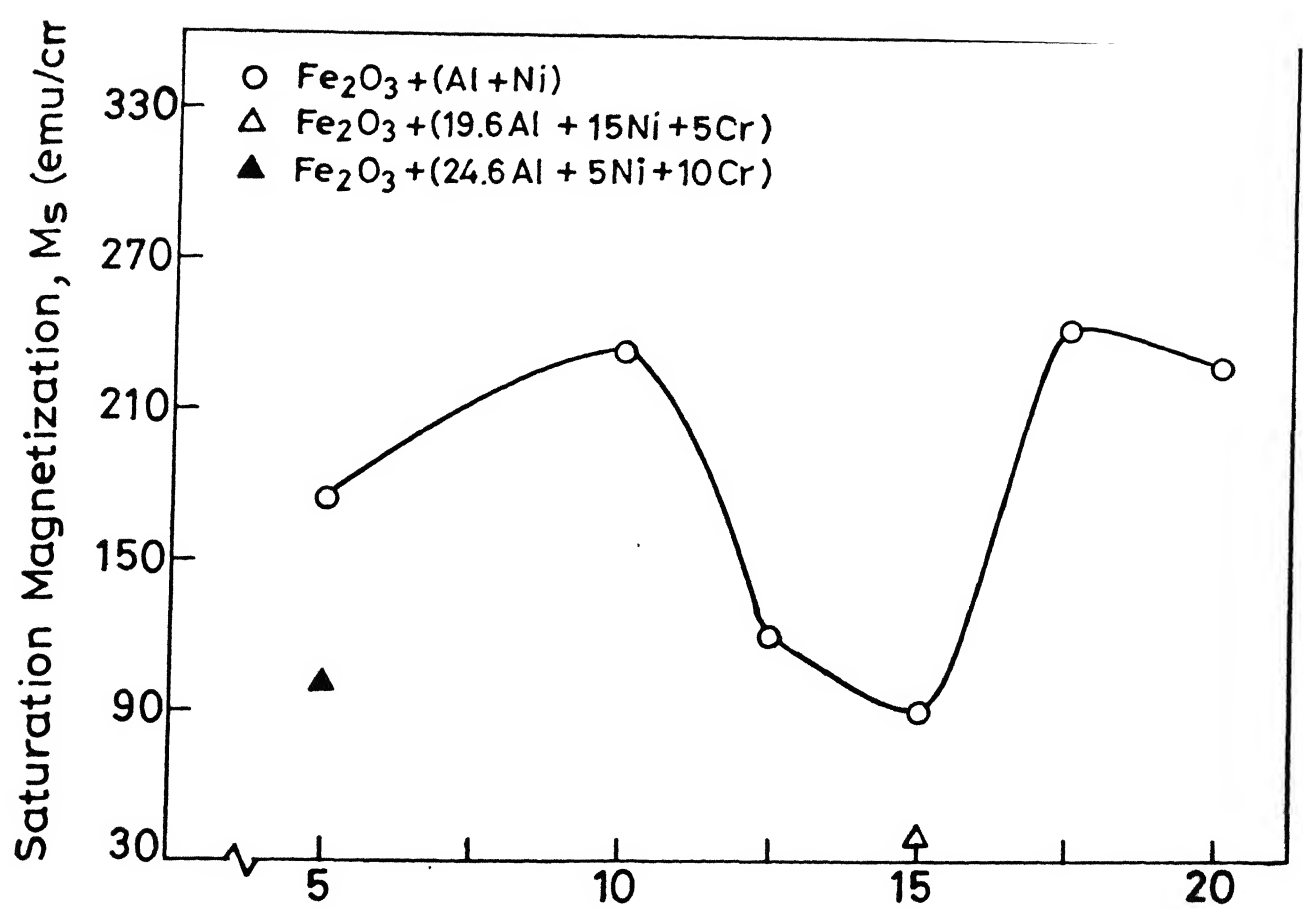


Fig.4.6 Variation of  $M_s$  and  $M_r$  with Vol % additive in  $\text{Al}_2\text{O}_3$ -Fe/Ni cermet.

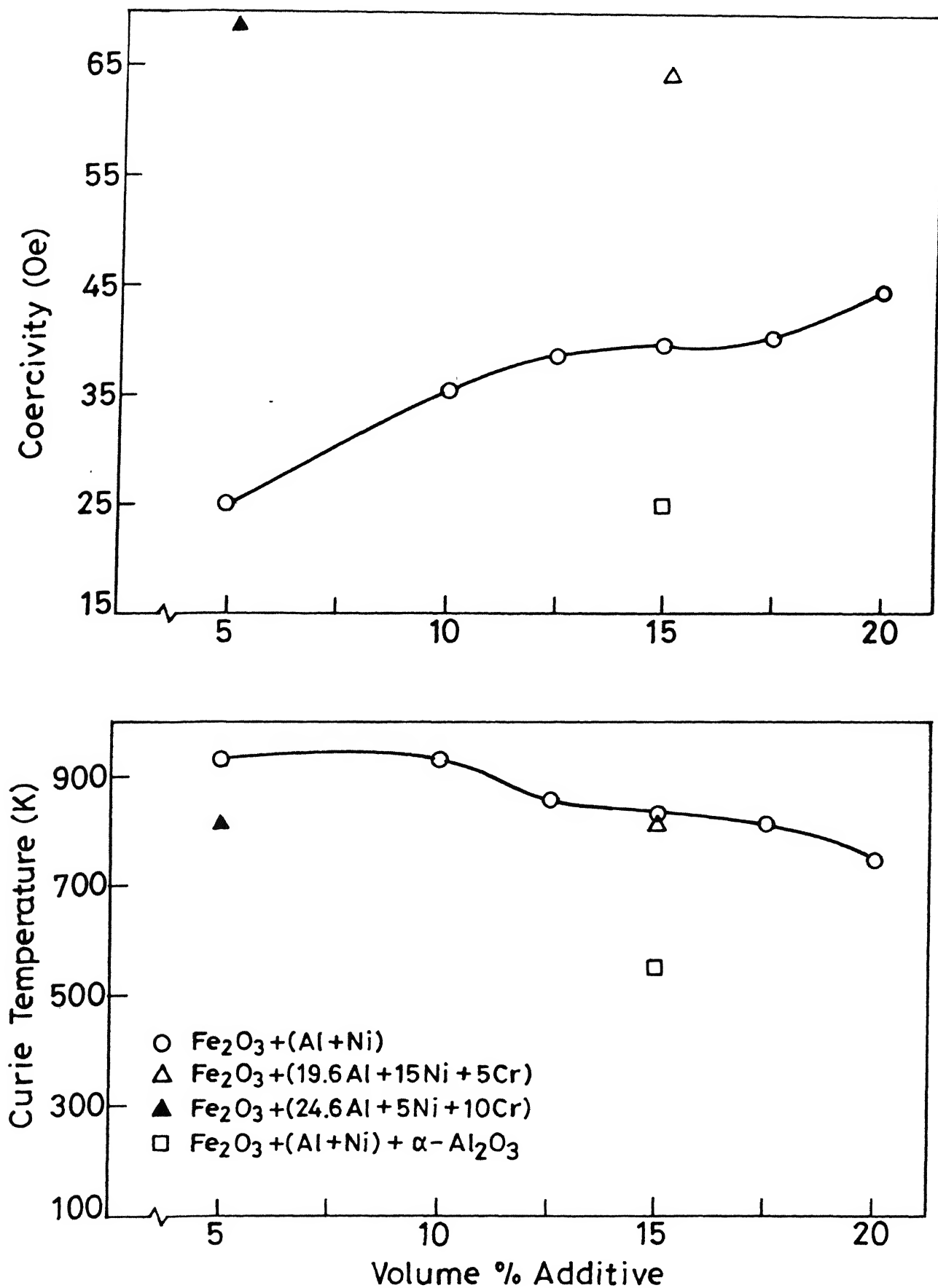


Fig.4.7 Variation of coercivity and curie temperature with Vol % additive in Al<sub>2</sub>O<sub>3</sub>-Fe/Ni cermet

There is no change in remanent magnetization at the composition 24.77 wt% Ni with 6.672 wt% Cr. But there is slight increase in the value at the composition 8.78 wt% Ni with 15.60 wt% Cr possibly some homogenization in the microstructure.

**Table 4.4 : Variation of Magnetization behaviour and curie temperature with vol% additive in  $\text{Al}_2\text{O}_3$ -Fe/Ni cermet**

Composition (wt%)				Saturation Magnetization ( $M_s$ ) emu/cm <sup>3</sup>	Remanent Magnetization ( $M_r$ ) emu/cm <sup>3</sup>	Coercivity ( $H_c$ ) Oe	Curie Temp. K
$\text{Fe}_2\text{O}_3$	Al	Ni	Cr				
74.73	25.26	-	-	-	-	-	-
69.64	20.56	9.79	-	175.17	6.29	25	930
65.19	16.47	18.33	-	232.48	5.48	36	930
63.16	14.61	22.21	-	120.46	2.93	37	860
61.28	12.86	25.85	-	90.18	2.56	39	830
59.48	11.22	29.28	-	272.29	2.19	41	820
57.80	9.66	32.52	-	227.28	2.31	44	750
58.72	9.82	24.77	6.67	38.96	2.26	64	820
62.48	13.11	8.78	15.60	102.10	4.41	67	815
*61.27	12.86	25.85	-			26	550

\* 2 wt%  $\alpha$  -  $\text{Al}_2\text{O}_3$  has also been added.

#### 4.10.3 Coercivity :

It is the field required to completely demagnetize the material, higher the field required to demagnetize, higher is the coercivity. The value of coercivity dictates whether the material is magnetically soft or hard. It is observed from the figure 4.7 that the increasing amount of wt% Ni increases the coercivity.

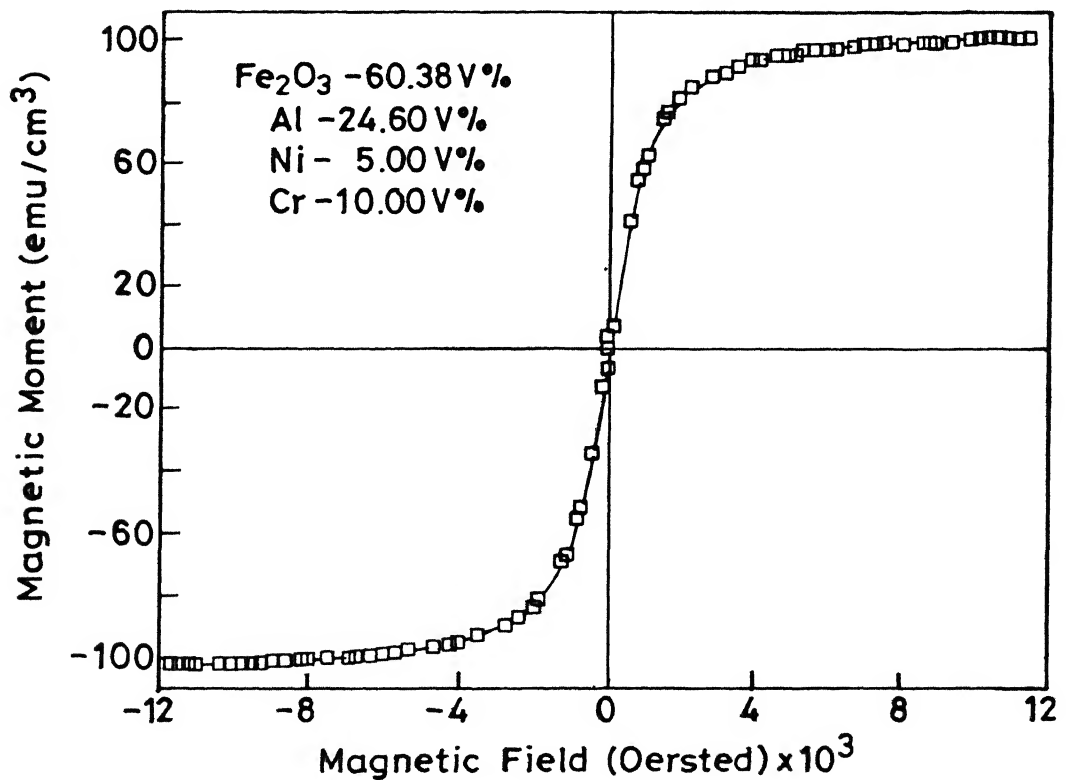
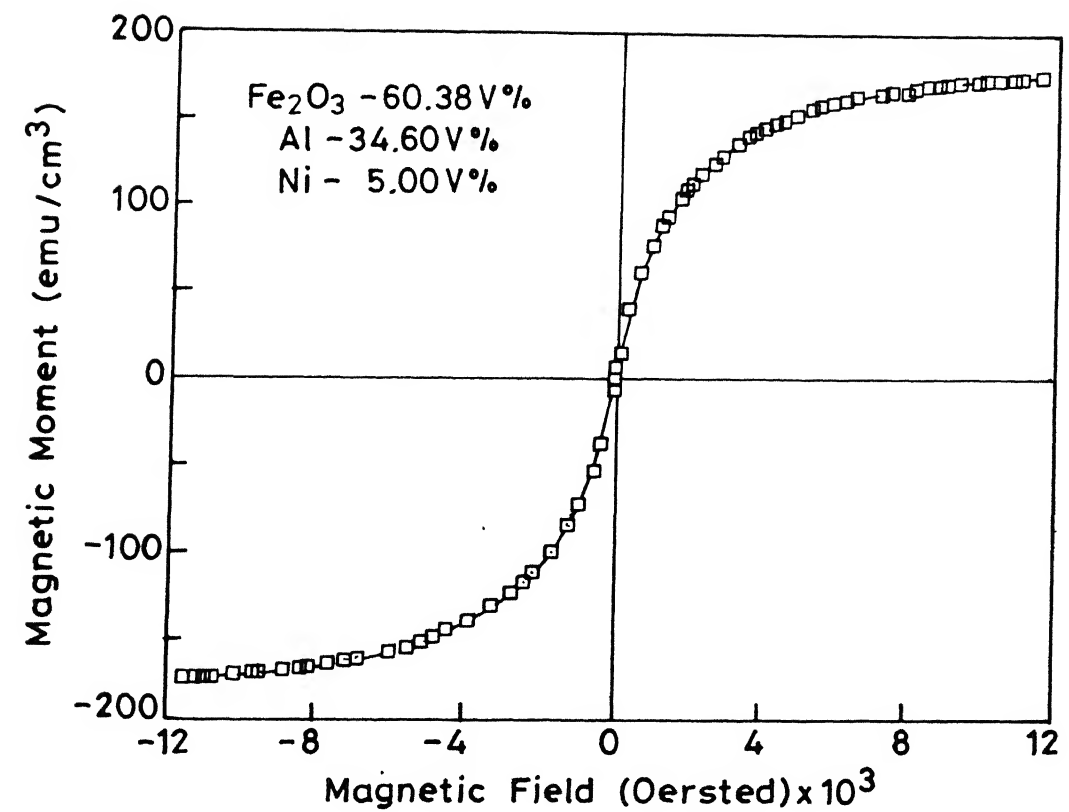


Fig.4.8 Effect of vol % additive on the (M-H) loop in  $\text{Al}_2\text{O}_3$  Fe/Ni cermet.

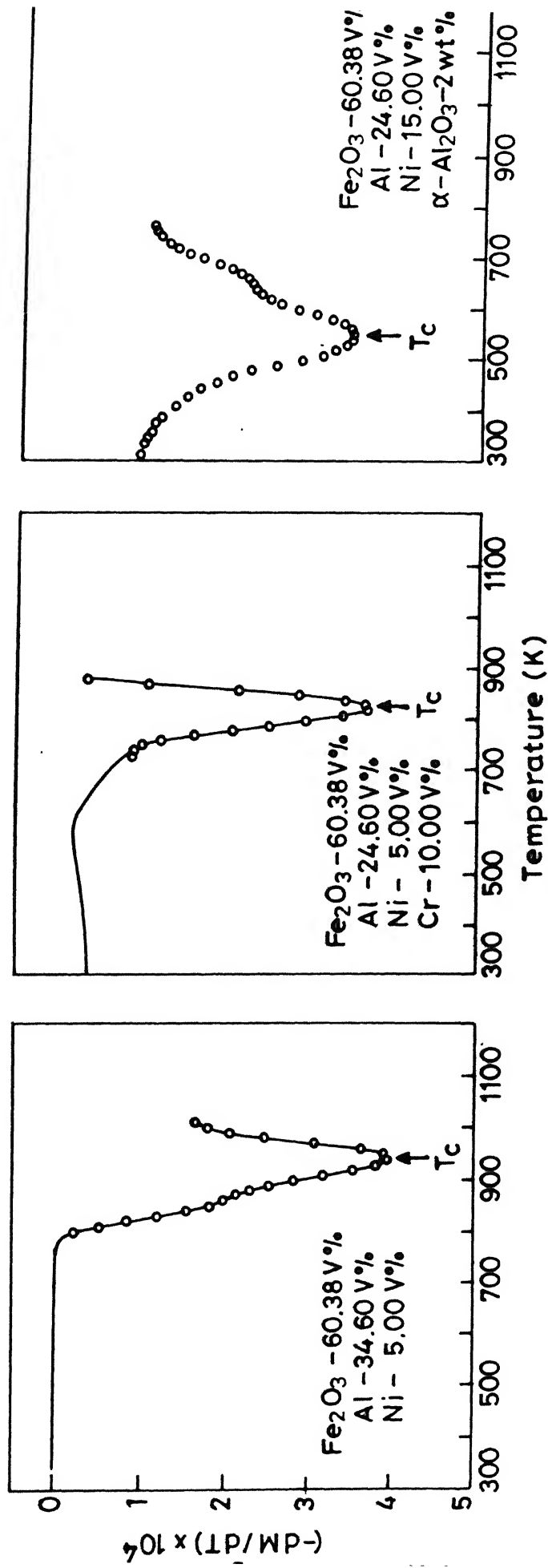


Fig.4.9 Variation of derivative magnetic moment with temperature in  $\text{Al}_2\text{O}_3$ -Fe/Ni cermet.

The increasing amount of wt% Ni has hindered the domain wall movement and has increased the coercivity. However, with the addition Cr the coercivity values are found to be increased. This is possibly the formation of  $\text{AlFe}_3\text{C}_{0.5}$ .

The principle of the modern inclusion theory as enunciated by Neel [54] and some modification in the above theory has been taken up later on in order to account for the non magnetic inclusions such as  $\text{AlFe}_3\text{C}_{0.5}$  in the ferromagnetic matrix. Goodeugh [55] has discussed the effect of inclusion or precipitates (causing reversal magnetization) on the coercive forces in polycrystalline ferro magnetic materials. His prediction indicates that  $H_C$  should increase with  $2/3$  power of volume of granular inclusions. For laminar precipitates  $H_C$  should increase linearly with the precipitate volume. The effect of shape and size of inclusion, second phase on  $H_C$  has also been considered. This theory nicely fits with our experimentally observed coercivity values. With the addition of 2 wt%  $\alpha\text{-Al}_2\text{O}_3$  in 25.85 wt% Ni a decrease in coercivity value is observed which is contrary to the modern 'inclusion' theory. Further work is required for its correct explanation.

#### 4.10.4 Hysteresis Curve (M-HD) :

In all the samples it is observed from the Fig. 4.8 that the energy losses are very very low and it approaches almost zero. The possible reason is the formation of small crystallite sizes, as determined by Scherres formula [47] from the XRD data. The variation of composition do not any substantial amount of change in the nature of hysteresis loop. The materials may find its application as a recording head of the tape recorder, transformer



core etc. [56].

#### 4.11 CURIE TEMPERATURE :

It is observed from the figure 4.7 that there is no change in curie temperature upto 18.338 wt% Ni addition. The curie temperature is 930K which is close to silicon iron (960K) at this composition [57]. With the increasing amount of Nickel the curie temperature is found to be decreased. However, there is a dip in curie temperature value at 32.52 wt% Ni. The curie temperature is found to be 750K at this composition which is close to 78 permialloy [57]. The variations of derivative magnetic moment with temperature in  $Al_2O_3$ -Fe/Ni cermet is shown in Fig. 4.9.

The addition of 6.672 wt% Cr with 24.77 wt% Ni, 15.70 wt%Cr + 8.78 wt% Ni do not show any substantial change in the curie temperature. The curie temperature is found to be 820K and 815K respectively. The addition of 2 wt%  $\alpha - Al_2O_3$  in 25.85 wt% Ni has greatly reduced the curie temperature. This is possibly the formation of a new phase.

## CHAPTER 5

## CONCLUSION AND SUGGESTION FOR FUTURE WORK

Based on the result and discussion the following conclusions can be drawn :

1. It seems possible to prepare  $\text{Al}_2\text{O}_3$  - metal composite using exotherm reactive hot pressing.
2. The rod milled powders have a average particle size in the range ( 1.24  $\mu\text{m}$  to 2.53  $\mu\text{m}$ ).
3. DTA confirms the exothermic reaction and endothermic reaction temperature with volume% additive in powder composition.
4. XRD is used for the identification of the phases and also the crystallite size with volume% additive in  $\text{Al}_2\text{O}_3$ -Fe/Ni cermet.
5. Variation of sintered density with vol% additive is observed in  $\text{Al}_2\text{O}_3$ -Fe/Ni cermet. There is a increase in the sintered density with the increasing amount of Nickel addition upto 12.5 vol% but at 15 vol% and 20 vol% Ni there is decrease in sintered density possibly the formation of a low density defect lattice. Aluminium Nickel (AlNi).Cr addition increases the sintered density.
6. Indentation hardness increases with vol% additive upto 12.5 vol% Ni and again at 20 vol% Ni but lower values are observed at 15 and 17.5 vol% Ni. As no solid solutions of (Fe, Ni)  $\text{Fe}_2\text{O}_4$  are observed with the 15 and 17.5 vol% Ni composition. The additions of Cr do not improve the hardness 2 Wt%  $\alpha$  -  $\text{Al}_2\text{O}_3$  addition also does not improve the hardness.
7. The samples containing 5, 10, 15, 20 vol% Ni showing similar TRS values. These samples exhibit microstructure of uniform grain size due to the presence of free Nickel. However, in contrast the samples containing 12.5 and 17.5 vol% Ni exhibit exaggerated grain growth due to absence of free Ni. Additions of Cr do not improve the TRS value whereas  $\alpha$ - $\text{Al}_2\text{O}_3$  addition shows the improvement in TRS value.
8. The values of saturation magnetization ( $M_s$ ) and remnant magnetization ( $M_r$ ) are low. The M-H loop area is quite low inspite of the variation of compositions in  $\text{Al}_2\text{O}_3$ - Fe/Ni cermet.

9. Curie temperatures are found to vary with vol% additive in  $\text{Al}_2\text{O}_3$ -Fe/Ni cermet.

**SUGGESTION FOR FUTURE WORK :**

1. The sintering temperature should be increased for the reduction of  $\text{Fe}_2\text{O}_3$  by Al, in presence of the additives (Ni, Cr), to form  $\text{Al}_2\text{O}_3$  - metal composites.
2. The hot pressing pressure should be increased to increase the sintered density and to decrease the porosity. The sintered density should be close to theoretical density.
3. The milling of powders should be uniform for better homogenization.
4. The additives (Ni, Cr) should cover the oxide particles and the Al particles properly.
5. Soaking time should be increased and the temperature at the sintering temperature should be properly controlled.
6. From the XRD data, lattice parameters of each set of compositions should be traced out and the theoretical density of the sintered pellets should be found out.
7. Proper choice of etchant should be made to observe the polished surface under SEM.
8. EDAX for each set of compositions should be done to obtain the distribution of each phases in the sintered pellets.

## REFERENCES

1. A. W. Espelund 'Aluminothermic reduction' Journal of Chemical Education, June 1975, Vol. 52, Number 6, pp 400-402.
2. Yokham, International Journal of self propagating High-Temp synth, 1992, 1(1), 161-7 (Eng).
3. Uilame. Umbelino Gomes, Angelus Guiseppe Pereira da Silva, Jose Nilson Franca de Holanda and Daltro Garcia Pinatli, 'Sintering of Nb-Tb powders from aluminothermic reduction product (ATR)', International Journal of Refractory Metals., Hard Materials, 1992, 11(1), 43-7 (Eng).
4. Yamada, Osamu, Miyamoto, Yoshinani, 'Fabrication of intermetallic compounds by advanced thermite type combination synthesis process' (Coll, Gen Educ, Osaka Ind Univ., Osaka Japan). Nippon Kinzoku Gakkushi, 1992, 56(8), 938-42 (Japan).
5. Odawara Osamu, 'Application of Combustion on research and development of metal-ceramic composite pipe-centrifugal thermite process', Grad Sch. Tokyo Int. Technol, Tokyo, Japan, Neusho Kenkyu, 1992, 89, 19-31 (Japan).
6. Odawara Osamu, 'Characteristics and development of centrifugal thermite process for fabrication of composite-structured pipes', (Grad Sch Nagatsuta Tokyo Int. Technology, Yokohama Japan 227) Nyu Seramikkusu, 1990, 3(6), 47-52 (Japan).
7. Takeda Synichi, 'Fabrication process of sintered ceramic material using heat of thermite reaction and control of their microstructure' (mater. Res. Lab., Komato Su Ltd., Hiratsuka, Japan 254) Nyuu Seramekkusu, 1990, 3(6), 73-9 (Japan).

8. Odawara Osamu, 'Metal-ceramic composite pipes produced by a centrifugal thermite process' (Dep. Electron Chem. Tokyo Int. Technol, Yokohama, Japan 227) Combnt. Plasma Synth. High-Temp Mater, 1990, 179-85 (Eng.) edited by Munir, zuhair A, Holt J. Birch, VCH, Newyork, NY.
9. Filatov, V. M., Naiboro Denko, Yu, S, (USSR), Khim, Fiz Protessov, Goreniya 'Vzruva, 'Effect of intermetallic reactions on combustion of nickel - aluminium thermit's' Mater 9 Vser Simp po Goreniyu i Vzryuu, Suzdal 19-24 (Noyab 1989 Chernigalovfea, 1989, 37-40 (Russ).
10. Zhukov, A. A, Novokhatsku V.A. Zhigutis Yu Yu (USSR) 'Preparation of cast tool steel by combination of thermite mixtures' Liteinoe Proizvod, 1990, 7(6).
11. Tada, Yoshihiro, Sato, Teisuke, 'Thermit reaction and mechanical properties of mechanically alloyed aluminium-metallic oxide composites (Eng coll Tokuyshima Univ., Tokushima Japan) Funtai cryats, Funmatsu Yakin 1989, 36(6) 677-82 (Japan).
12. Yamazaki Katsuhiro, (Komatsu Ltd.), 'Thermite process for metal composite preparation Jpn Kokai Tokkyo Koho Jp. 62, 253, 703 [87, 253, 703] (Cl B 22F 7/04) 05 Nov 1987, Appl 86/96, 884, 28 Apr 1986, 3pp.
13. Odawara Osamu, 'Joining of metals to ceramics by self propagating exothermic reaction Centrifugal thermite method' (Grad Sch Nagatshuda Toyko Int Technol Yokohama Japan 227) Soscitokoko 1987, 28(332) 1109-14 (Japan).

14. Sata Nobuhiro, Asano Osamu, 'Ceramic lining of metal pipes by thermite process' (Agency of industrial sciences and technology) Jpn Kokai Tokkyo Kiho Jp 63, 89, 679 [88, 89, 679] (C1 C23 C20/06) 20 Apr 1988 App 86/233, 779 01 Oct. 1986, 4 pp.
15. Sata Nobuhiro, Asano osamu, 'Ceramic lining of long steel tube by thermite process' (Agency of industrial science and Technology) Jpn Kokai Tokkyo Koho Jp, 63, 89680 [88, 89, 680] (C1 C 23 C20/06) 20 April 1988, Appl 86/233,780, 01 Oct. 1987, 3 pp.
16. Sata Nobuhiro, Asano Osamu, 'Ceramic lining of steel tubes by thermite process (Agency of Industrial Sciences and Technology) Jpn kokai Tokkyo Koho JP 63, 89677, [88, 89, 677] (C1 C 23, C20/06) 20 April 12988, Appl. 86/233, 277 01 Oct. 1986, 4 pp.
17. Sata Nobuhiro, Asano Osamu, 'Ceramic Coating on the innerwall of metal tube by thermite process' (Agency of Industrial Sciences and Technology) Jpn Kokai Tokkyo Koho Jp 6389, 676 [88, 89, 176] (C1 C23 C20/06) 20 April 1988, Appl 86/233, 176, 01 Oct. 1986, 3 pp.
18. Sata Nobuhiro, Asano Osamu, 'Ceramic lining of steel tubes by thermite process' (Agency of Industrial Sciences and Technology) Jpn Kokai Tokkyo Koho Jp 6389, 678 [88, 89, 678] (C1 C 23 C20/06) 20 April 1988, Appl 86/233, 778, 01 Oct 1986, 3 pp.

19. Filatov, V.M. Naiborodinko, Yu S (Tomsk USSR) Fiz Goreniya Vzryva 'Thermodynamic analysis of the combination of the low-gas system with a redox stage' 1988, 24/4), 98-101 (Russ).
20. Odawara, Osamu Ishii, Yasumarra, Yamazaki Hiroshi, Sato Mikio 'Manufacture of composite pipes' (Agency of Industrial Sciences and Technology Kubota Ltd.) Jpn, Kokai Tokkyo Koho JP 62, 86, 172 [ 8786, 172] (C1 C23 C20/00) 20Apr 1987, Appl 85/227, 603, 11 Oct. 1985 4pp.
21. Odawara Osamu, Ishii, Yasumora, Yamazaki Hiroshi, 'Manufacture of Composite pipes' (Agency of industrial Sciences and Technology Kubota Ltd.) Jpn, Kokai Tokkyo Koho Jp 6286, 173 [87, 86173] (C1 623 c20/00) 20 Apr 1987, Appl 85/227, 86173] (C1 C23 C20/00) 20 Apr. 1987, Appl. 85/227, 604, 11 Oct 1985, 5pp.
22. Ogata Masasu, 'Manufacture of ceramic metal joined body' (Komatsu Ltd.) Jpn Kokai Tokkyo Koho Jp 62, 148, 381 [87, 148, 381] (C1 C0413 37/02) 02 Jul 1987, Appl. 85/289, 461, 24th December 1985, 5 pp.
23. Takeda Shuichi, Shishiba Hideki, 'Silicon nitride sinter of high hardness and density' (Komat Su Ltd.) Jpn Kokai Tokkyo Koho Jp 62, 119, 166 (87, 119, 166) (C1 C04 B 35/58) 30 May 1987, Appl 85/255, 009, 15th Nov. 1985, 4 App.

24. Odawara Osamu, Ishu Yarumara, Yamazaki, Hiroshi, 'Lining of steel pipe by centrifugal thermite process' (Agency of Industrial Sciences and Technology, Kubota Ltd.) Jpn Kokui Tokkyo Koho Jp 61, 238, 974 [86, 238974] (C1 C23 C20/00) 24 Oct 1986, App 85/79, 577, 15 Apr 1985, 3pp.
25. Odawara Osamu, Ishu Yarumara, Yamazaki Hiroshi, 'Ceramic lined pipe' (Agency of Industrial Sciences and Technology Kubota Ltd.) Jpn. Kokai Tokkyo Koho Jp 61, 238, 975 [ 86, 238, 975] (C1 C 23 C20/00) 24 Oct 1986. Appl. 85/79, 57 15 Apr 1985, 5pp.
26. Sata Nubuhiko 'Fabrication of plate or tubular form ceramic materials by thermite reaction' (Agency of Industrial Sciences and Technology) Jpn Kokai Tokkyo Koho Jp 6227, 376 [87 27, 376] (C1 C04B 35/60) 05 Feb. 1987, Appl 85/162, 518 23 Jul. 1985, 4pp.
27. Park J.H., Jun B. S, Lee E.C., 'Synthesis of ceramic raw material using thermite ignition sialon formation' (Dep. Ceramic Eng. Youssi Univ. Seonl. S. Korea) Sprechsaal 1986, 119 (12) 1135-8 (Eng).
28. Ogata Marasu, Takeda Shuichi, 'Sintering process' (Komatsu Ltd.) PCT Int. Apl. No. 8604, 890 (C1 C04B35/64) 28 Aug. 1986, Jp. Appl 85/26, 424. 15 Feb. 1985, 22pp.
29. Odawara Osamu, Ishu Yarumara, Yamazaki Hiroshi, 'Ceramic lined composite pipes' (Agency of Industrial Sciences and Technology, Kubota Ltd.) Jpn. Kokai Tokkyo Koho Jp 61, 78 633 [86, 78633] (C1 B32 B1/08) 22 April 1986. Appl 84/202, 768, 27 Sep. 1984, 6pp.



30. Sismanis Paragiotis G Argyro Poulos Stavvon A, Deeley, Paul D  
 'The dissolution of microexothermic alloying to cast iron'  
 (Dep Min, Metall Engg. McGill Univ. Montreal, PQ Can H3A,  
 2A7) Electr. Furn. Conf. Proc. 1985 (Pub. 1986), 43, 39-55  
 (Eng.)
31. Gehrmaun Ebba, Frischat, Guinther H ' Vacuum centrifugal  
 thermite process for producing ceramic lined pipes' (Minist.  
 Int. Trade Ind. Guv., Ind. Res Tnst., Sendai Japan 983) J.  
 Am. Ceramic Soc. 1986, 69(4) C85-C86 (Eng.)
32. Merzhanov A.G. Yukhvid V.I. Borovimko, I.P. Deev V. V.  
 Ershev, Yu V, Toropov V. M. Timokhin, N.N. 'Mullilayer shell  
 investment molds' (USSR) Su 1, 205, 986 (Cl B22 C9/04), 23  
 Jan 1986, Appl 3, 476, 796, 30 Jul 1982. From offcnytfiy  
 Izobret 1986 (3) 41.
33. Odawara, Osamu, Yamazaki, Hiroshi 'Additives for thermal  
 enamelling agents for metal tubes' (Agency of Industrial  
 Sciences and Technology, Kubota Ltd.) Jpn Kokai Industrial  
 Sciences and Technology Kubota Ltd., Jpn Kokai Tokkyo Koho JP  
 60, 217, 140 [85, 217, 140].
34. Odawara, Osamu, Shiraishi Mara, Ikenchi, Jun Ishu, Yarumara,  
 Yamaraki, Hiroshi, Sato Mikio, 'Characteristics of thermit  
 raction in a centrifugal thermit process' (Gov. Ind. Res.  
 Inst. Sendai Japan) Nippon Kinzoku gokkaishi 1995, 49(9),  
 806-10 (Japan).
35. Janiku. Stefan, 'Development of alumino thermic welding  
 technology in the building industry' (Czech) Zvaracske Spravy  
 1985, 35(1) 1-10 (Eng/Slo).

36. 'Formation of acid resistant ceramic on the inner surface of concrete pipes' Agency of Industrial Sciences and Technology Kukota ltd. Mitsubishi, Mining and Cement Co., Ltd. Jpn Kokai Tokkyo Koho Jp, 59, 232, 8071 (C1 B28B21/72) 27 Dec. 1984, Appl. 83/107, 281 15 June 1983, 4pp.
37. Feichtinger, Heinrich K, Rascheeff Nikolai W, 'Powdered material for oxidation and heat resistant layers linings and shape bodies and apparatus for applying this material' PCT Int. Appl. No. B501, 79/C1 H05B7/12) 14 March 1985, CH Appl 83/4601, 24 Aug. 1983, 26 pp.
38. Kaluba Wldzimierz, Jozwiak Karol, Kachlicki Tomarz, 'Structural analysis of chromium diffusion layers prepared on steel 45 by the aluminothermic method (Politech Poznanska, P{oznan, Pol) Mater. Konf-konf Mitrosk. Electron Ciala Stalego 6th 1981, 270-3 (Pol) Akad Gorn - Hutn im S. Staszica Krakow pol.
39. 'Cermets' Pagenoz edited by J R Tink Iepangh and W.B. Crandall, 1960 Reinhold publishing Corporation, New York.
40. H. Partor 'Present Status and development of tool materials: Part 1 Cutting tools' (Ugicarb Morgon, 54, Avenue Rhin et Danube 38100 Grenoble, France) Journal of Refractories and Hard Material, December 1987.
41. R. L. Cobles, 'Reactfine sintering' published in materials science manographs, 14, Sintering theory and practice edited by D. Kolar S. Pejovnik and M.M. Ristic, printed in Elesvier Scientific Publishing Company, 1982.

42. W.D. Kingery, H. K. Bowen and D. R. Uhlmann, Introduction to ceramics, second ed., J. Wiley and Sons, New York, 1976.
43. A. E. Paladino and E. Magure, J. Am. Ceram. Soc. 53 [2] (1970), 98.
44. Milivoj K. Burn and Minyoung Lee 'Reactive hot pressing studies of high density oxide-carbide composite 'ceramics', International Journal of Refractory metals and Hard Materials II, (1992), 75-82.
45. A.C.D. Chaklader and M. N. Shetty 'Ceramic - Metal composites by Reactive Hot pressing' Transaction of the Metallurgical Society of AIME, July 1965, Vol. 233, 1440-1442.
46. Differential thermal analysis edited by R. C. Mackenzie, Vol. 1, 1970, Academic Press.
47. Elements of X-Ray Diffraction by B. D. Cullity, 2nd edition. 1978, Addison-Wesley Publishing Company, INC.
48. J. H. Chesters 'Steel plant refractories', The United Steel Companies Ltd., Sheffield, 1963, 2nd ed. pp. 680-86.
49. 1984 Annual Book of ASTM Standards Section 3 'Metals Test Methods and Analytical procedures, Vol. 0.3.01: Metals-Mechanical Testing, Elevated and Low temperature Tests, pp. 795, Designation E855-84.
50. Mechanical metallurgy by Georg E. Dieter and David Bacon, McGraw-Hill Book Company, 1988.
51. Materials Science Part - III by Manas Chanda, 1979, pp 127-154.
52. Ceramic Microstructures edited by Richard M. Fulrath and Joseph A. Park. John Wiley and Son Inc.

53. Introduction to magnetic materials by B.D. Cullity, Addison-Wesley Publishing Company.
54. L. Neel, Analysis of Grenoble University, 1948, 22, p. 299.
55. John B. Goodenough, Phy. Review, 1954, 95, 917.
56. Olson, R.D. 'Application of Softmagnetic materials and Speciality alloys', J. Apply Phys., 1966, 37, 1197-1201.
57. Ferromagnetism by Richard M. Bozorth, 5th printing, D. Van Nostrand Company, Inc, Princeton, New Jersey.

A

119345

MME-1995-M-CHA-PRO